Supplement for:

Resolving ecological feedbacks on the ocean carbon sink in Earth system models

David I. Armstrong McKay*[1,2], Sarah E. Cornell[1,2], Katherine Richardson[3], Johan Rockström[1,4]

1 Stockholm Resilience Centre, Stockholm University, SE-10691, Sweden

2 Bolin Centre for Climate Research, Stockholm University, SE-10691, Sweden

3 Globe Institute, Center for Macroecology, Evolution and Climate, University of Copenhagen, Denmark

4 Potsdam Institute for Climate Impact Research, Potsdam, Germany

*david.armstrongmckay@su.se

1. cGEnIE–ecoGEnIE default and recalibration parameters

Table S1: Key parameter values used for default and recalibrated cGEnIE–ecoGEnIE configurations. The primary calibration goal was equivalent biological pump strengths and similar initial carbonate chemistry (% difference with BIO+FPR default configuration given for each other configuration parameter).

Parameter	**BIO+FPR (default)**	**BIO+TDR**		**ECO+FPR**		**ECO+TDR**	
		Default	**Recalib.**	**Default**	**Recalib.**	**Default**	**Recalib.**
POC global export (PgC y^{-1})	7.503	8.042	7.503 *(0%)*	11.331	7.503 *(0%)*	10.995	7.503 *(0%)*
PIC global export(PgC y^{-1})	0.995	1.074	0.994 *(-0.1%)*	0.896	0.994 *(-0.1%)*	0.874	0.995 *(0%)*
POC global rain (sedimentation) (PgC y^{-1})	0.696	0.669	0.885 *(+27%)*	1.045	2.884 *(+314%)*	1.455	2.854 *(+310%)*
PIC global rain (sedimentation) (PgC y^{-1})	0.561	0.604	0.558 *(-0.5%)*	0.542	0.602 *(+7.3%)*	0.527	0.603 *(+7.5%)*
Surface [CO_2] (µmol kg^{-1})	24.05	25.1	27.11 *(+13%)*	40.0	29.51 *(+23%)*	51.2	28.17 *(+17%)*
Surface [CO_3] (µmol kg^{-1})	105.5	101.6	97.6 *(-7.5%)*	78.9	103.6 *(-1.8%)*	70.0	104.4 *(-1.0%)*
Surface [HCO_3] (µmol kg^{-1})	2091.5	2101.6	2111.8 *(+1.0%)*	2164.3	2094.6 *(0.1%)*	2191.5	2086.2 *(-0.3%)*
Total DIC (µmol kg^{-1})	2221.1	2228.3	2236.2 *(+0.7%)*	2283.3	2227.7 *(+0.3%)*	2312.7	2218.8 *(-0.1%)*
Total ALK (µmol kg^{-1})	2363.4	2363.2	2363.2 *(0%)*	2371.1	2386.9 *(+1.0%)*	2377.2	2376.6 *(+0.6%)*

2. Model validation against data

2.1. Dissolved Inorganic Carbon (DIC) in cGEnIE & ecoGEnIE versus observations

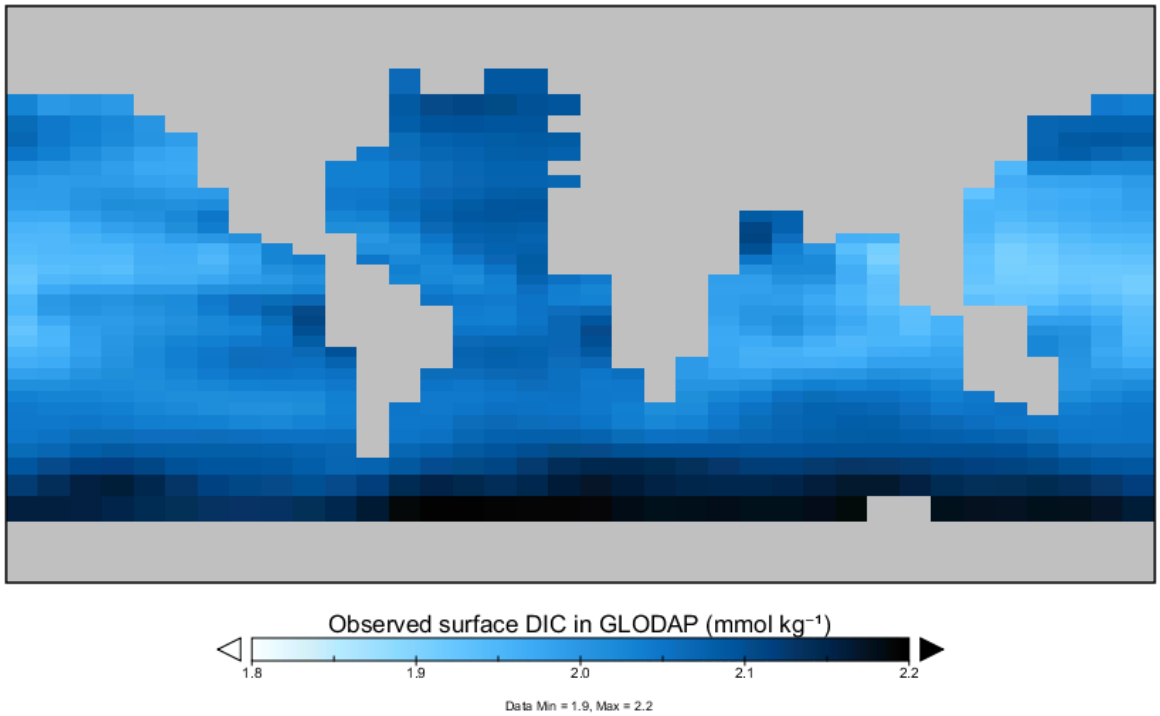

Figure S1: Map illustrating observed surface Dissolved Inorganic Carbon (DIC) in re-gridded GLODAPv2 data (Olsen et al., 2016; Ward et al., 2018). Plot created with Panoply, available from NASA Goddard Space Flight Center.

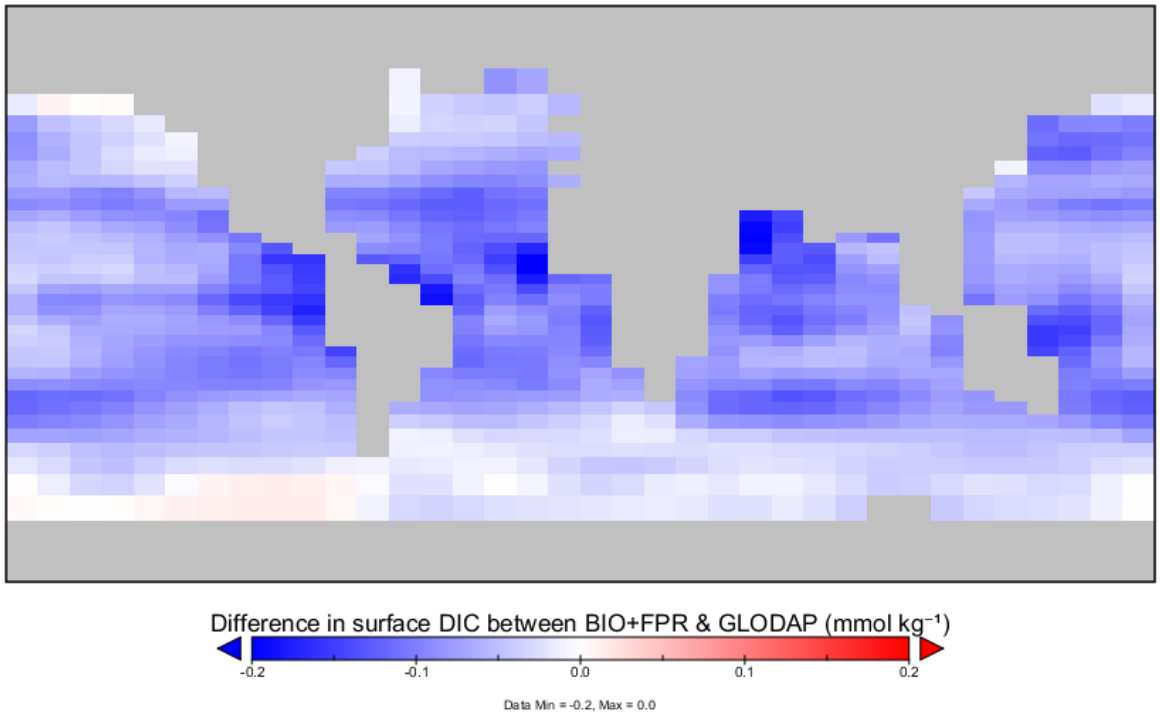

Figure S2: Map illustrating difference in surface DIC between BIO+FPR and re-gridded GLODAPv2 data (Olsen et al., 2016; Ward et al., 2018). BIO+FPR DIC is in general less than observed in subpolar waters, but the difference is not substantial relative to the global mean (~2 mmol kg^{-1}). Plot created with Panoply.

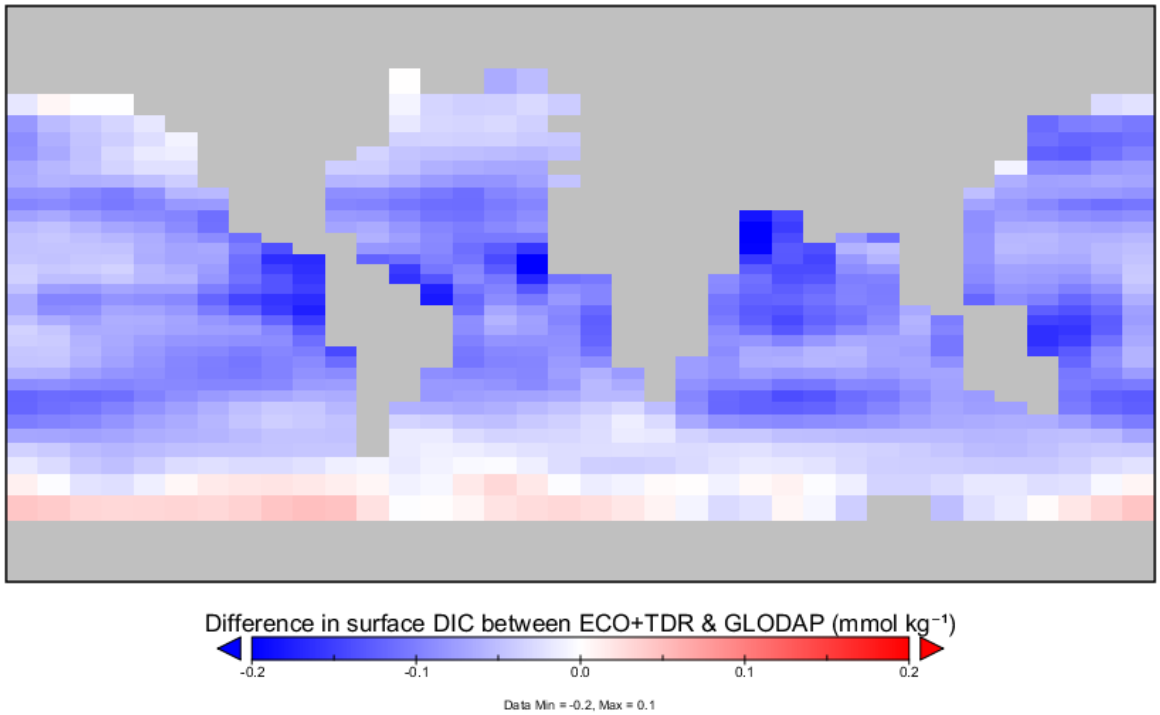

Figure S3: Map illustrating difference in surface DIC between our recalibrated ECO+TDR and re-gridded GLODAPv2 data (Olsen et al., 2016; Ward et al., 2018). ECO+TDR DIC is in general less than observed in low and mid-latitude waters and higher in the Southern Ocean, but the differences are not substantial relative to the global mean (~2 mmol kg^{-1}) or BIO+FPR. Plot created with Panoply.

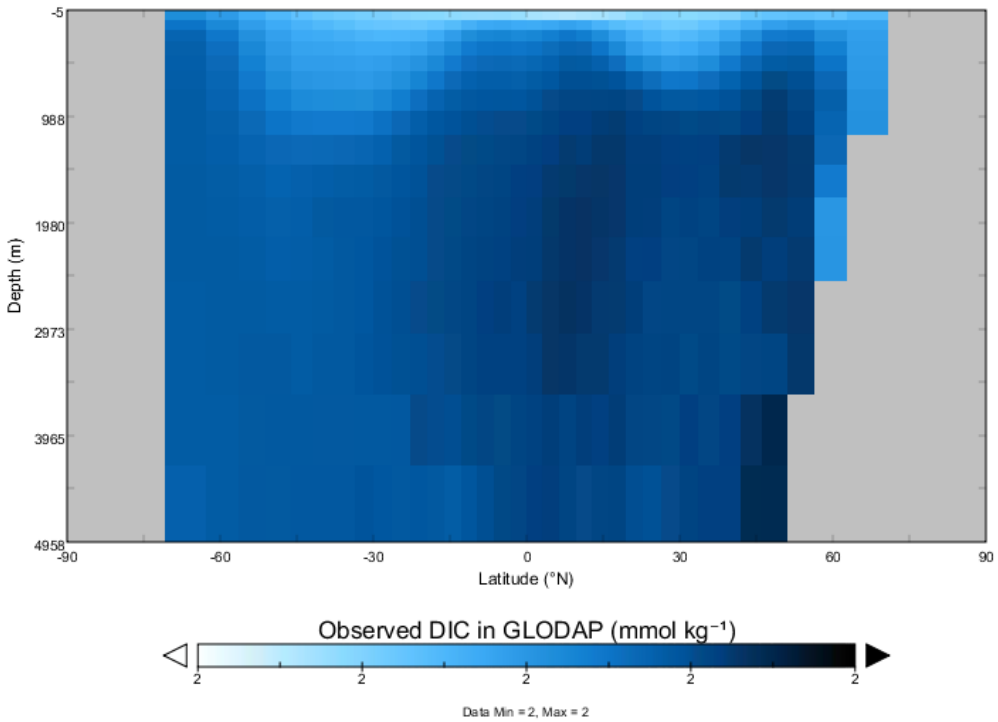

Figure S4: Depth plot illustrating observed DIC in re-gridded GLODAPv2 data (Olsen et al., 2016; Ward et al., 2018). Plot created with Panoply.

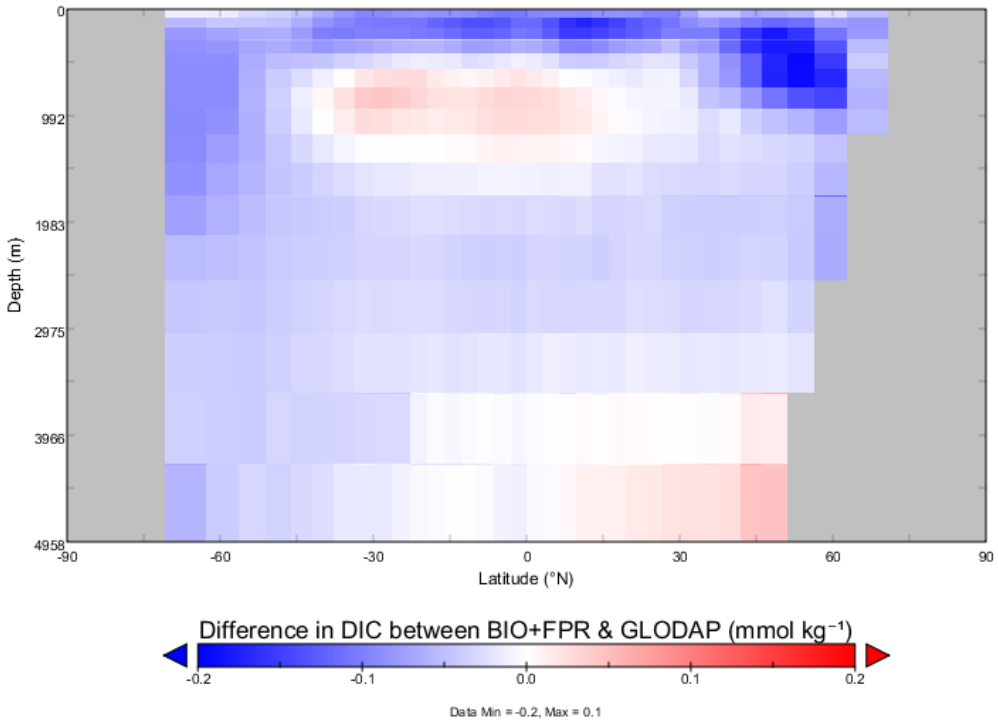

Figure S5: Depth plot illustrating difference in DIC between BIO+FPR and re-gridded GLODAPv2 data (Olsen et al., 2016; Ward et al., 2018). BIO+FPR DIC is in general less than observed at most depths and more than observed in intermediate low latitudes and deep Northern latitudes, but the difference is not substantial relative to the global mean (~2 mmol kg^{-1}). Plot created with Panoply.

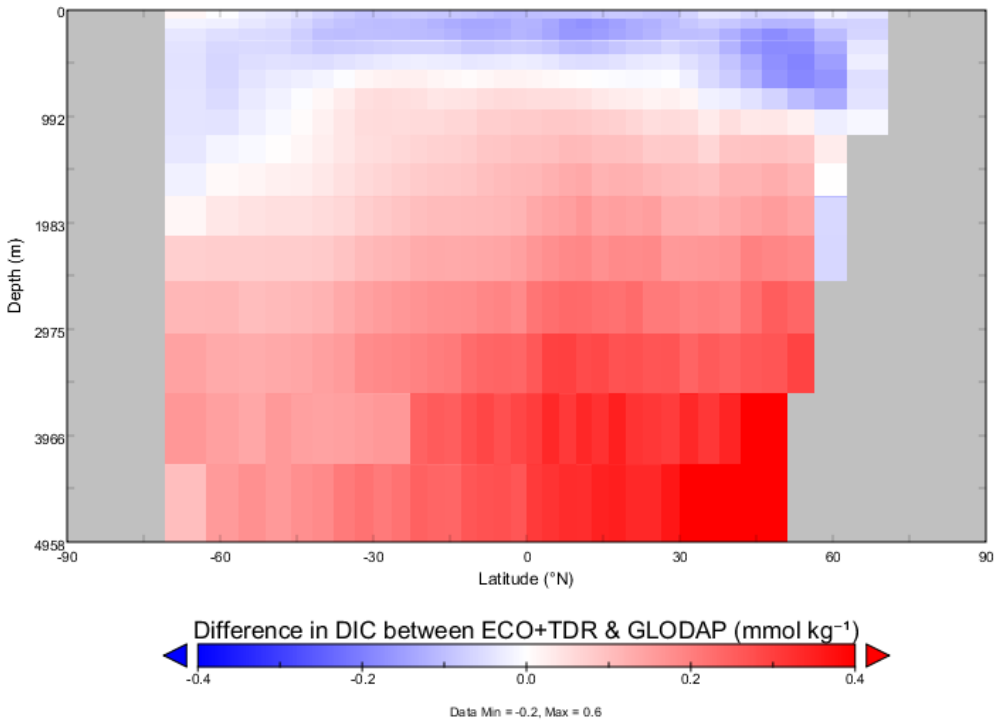

Figure S6: Depth plot illustrating difference in DIC between our recalibrated ECO+TDR and re-gridded GLODAPv2 data (Olsen et al., 2016; Ward et al., 2018). ECO+TDR DIC is in general less than observed in shallow waters and higher in deeper waters, but apart from the deep Northern ocean the difference is not substantial relative to the global mean (~2 mmol kg^{-1}). Higher deep water DIC relative to BIO+FPR is driven by elevated POC recalcitrant fraction in the ECO+TDR calibration which is remineralised at the ocean floor. Plot created with Panoply.

2.2. *Alkalinity (ALK) in cGEnIE & ecoGEnIE versus observations*

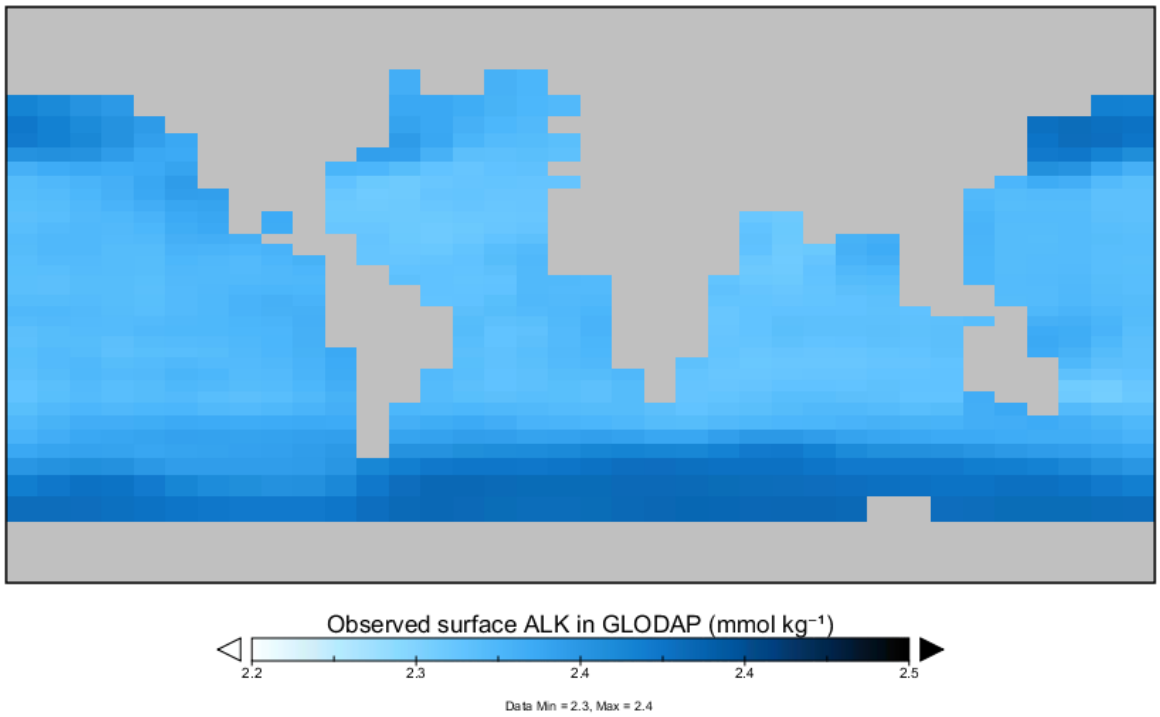

Figure S7: Map illustrating observed surface potential alkalinity (ALK) in re-gridded GLODAPv2 data (Olsen et al., 2016; Ward et al., 2018). Plot created with Panoply.

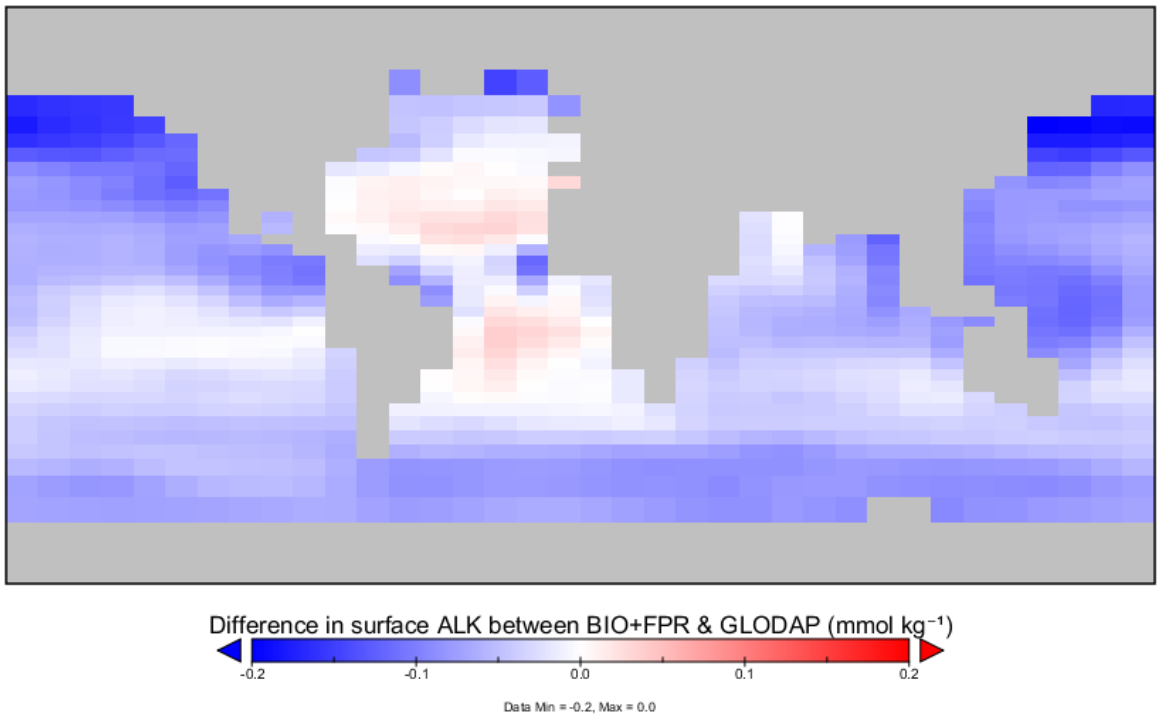

Figure S8: Map illustrating difference in surface ALK between BIO+FPR and re-gridded GLODAPv2 data (Olsen et al., 2016; Ward et al., 2018). BIO+FPR ALK is in general more than observed within the Atlantic and less than observed beyond (a pattern reflecting a slightly reduced range in salinity relative to observations), but the difference is not substantial relative to the global mean (~2.3 mmol kg^{-1}). Plot created with Panoply.

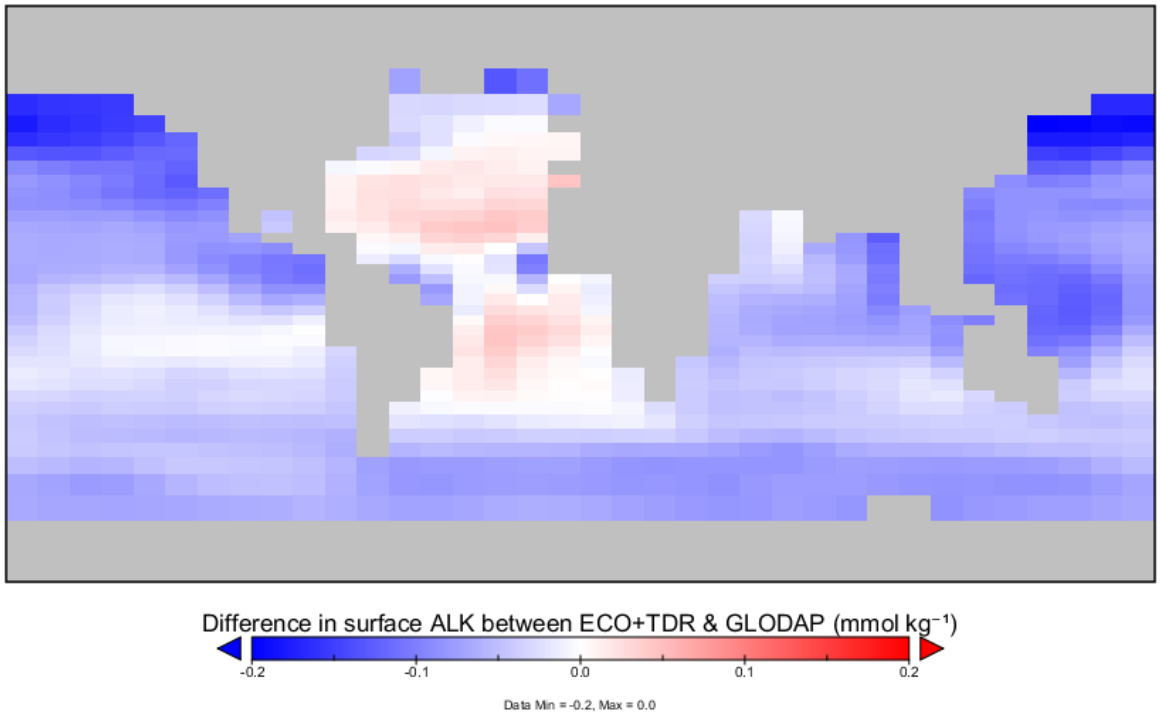

Figure S9: Map illustrating difference in surface ALK between our ECO+TDR and re-gridded GLODAPv2 data (Olsen et al., 2016; Ward et al., 2018). ECO+TDR ALK is in general more than observed within the Atlantic and less than observed beyond (a pattern reflecting a slightly reduced range in salinity relative to observations), but the difference is not substantial relative to the global mean (~2.3 mmol kg^{-1}) or the BIO+FPR configuration. Plot created with Panoply.

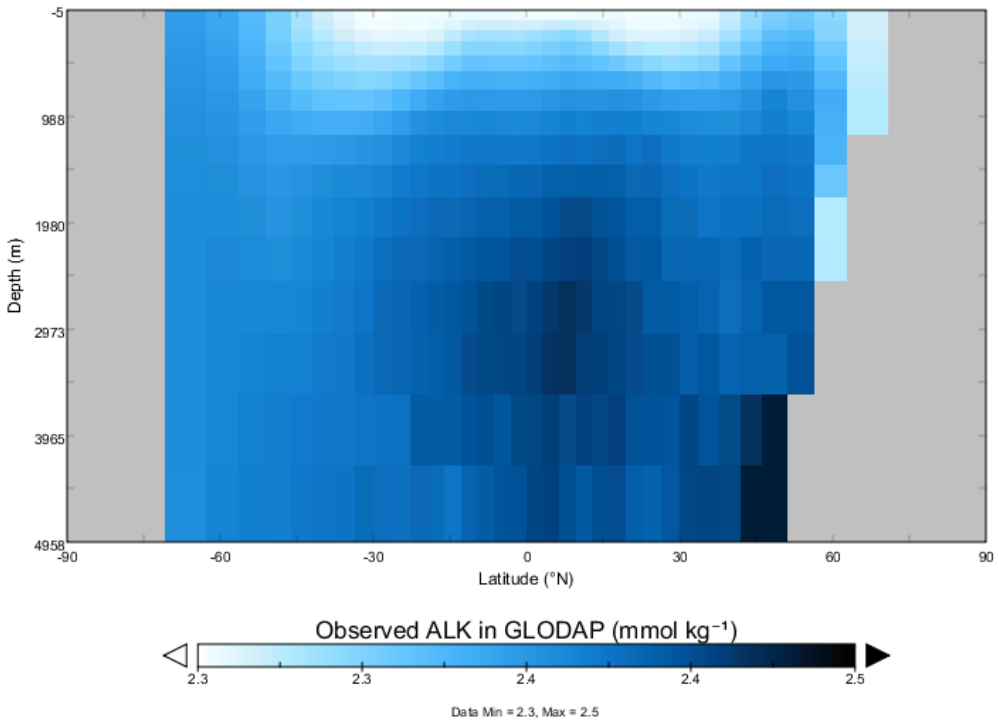

Figure S10: Depth plot illustrating observed potential alkalinity (ALK) in re-gridded GLODAPv2 data (Olsen et al., 2016; Ward et al., 2018). Plot created with Panoply.

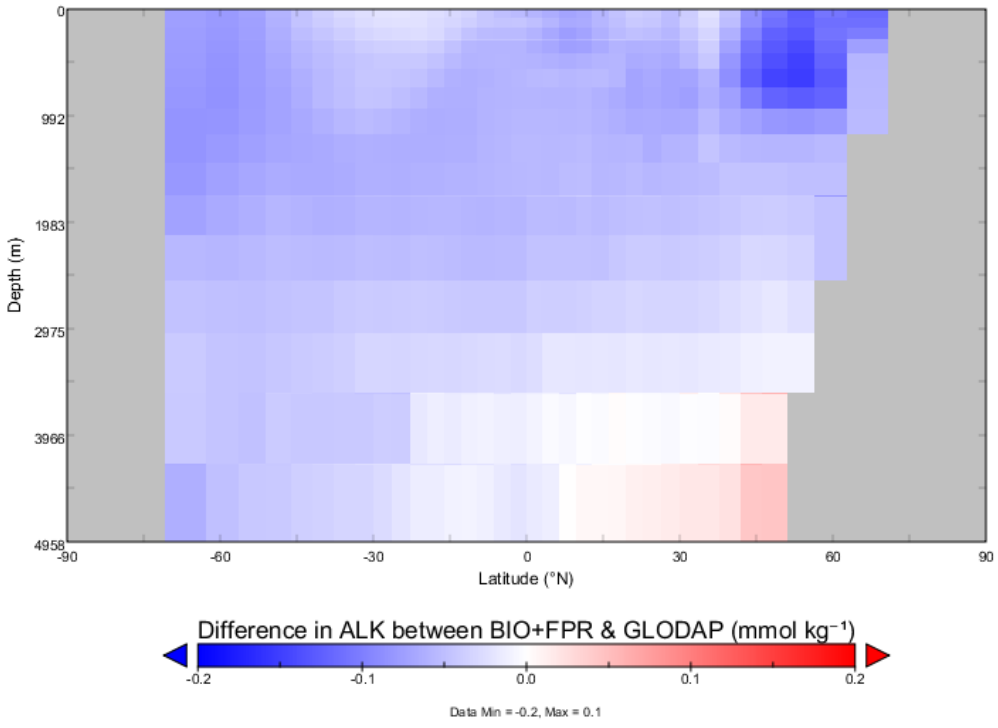

Figure S11: Depth plot illustrating difference in ALK between BIO+FPR and re-gridded GLODAPv2 data (Olsen et al., 2016; Ward et al., 2018). BIO+FPR ALK is in general less than observed apart from higher values in the deep Northern ocean, but the difference is not substantial relative to the global mean (~2.3 mmol kg^{-1}). Plot created with Panoply.

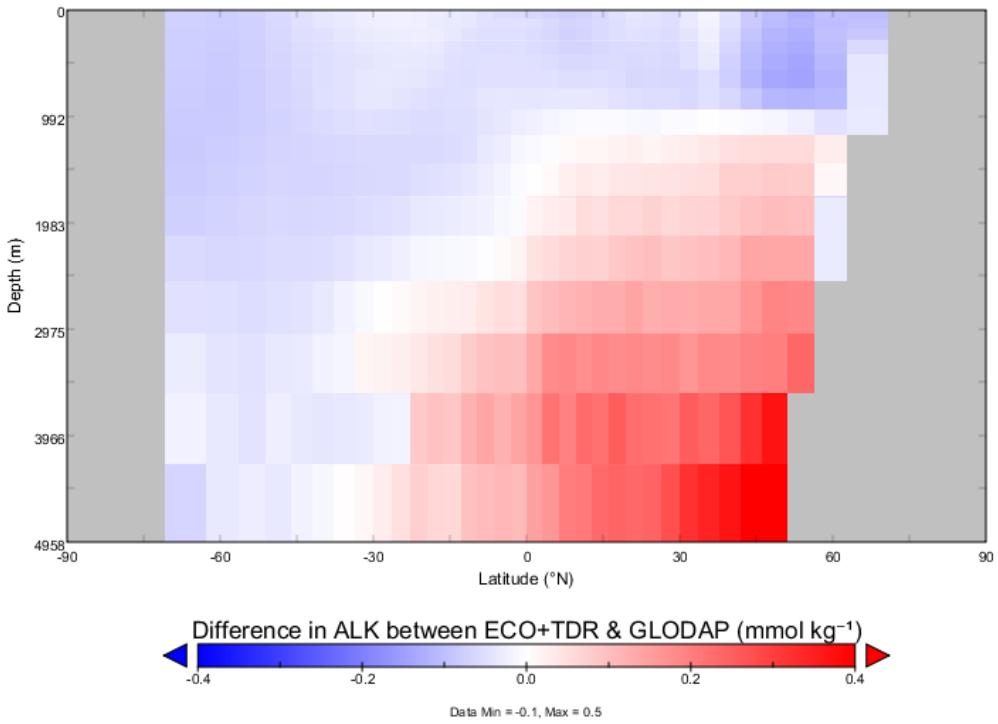

Figure S12: Depth plot illustrating difference in ALK between our recalibrated ECO+TDR and re-gridded GLODAPv2 data (Olsen et al., 2016; Ward et al., 2018). ECO+TDR ALK is in general less than observed apart from the deep Northern ocean, but the difference is mostly not substantial relative to the global mean (~2.3 mmol kg^{-1}). Higher deep water ALK relative to BIO+FPR is driven by elevated PIC sedimentation which is remineralised at the ocean floor. Plot created with Panoply.

2.3. *Chlorophyll and Phosphate (PO_4) in cGEnIE & ecoGEnIE versus observations*

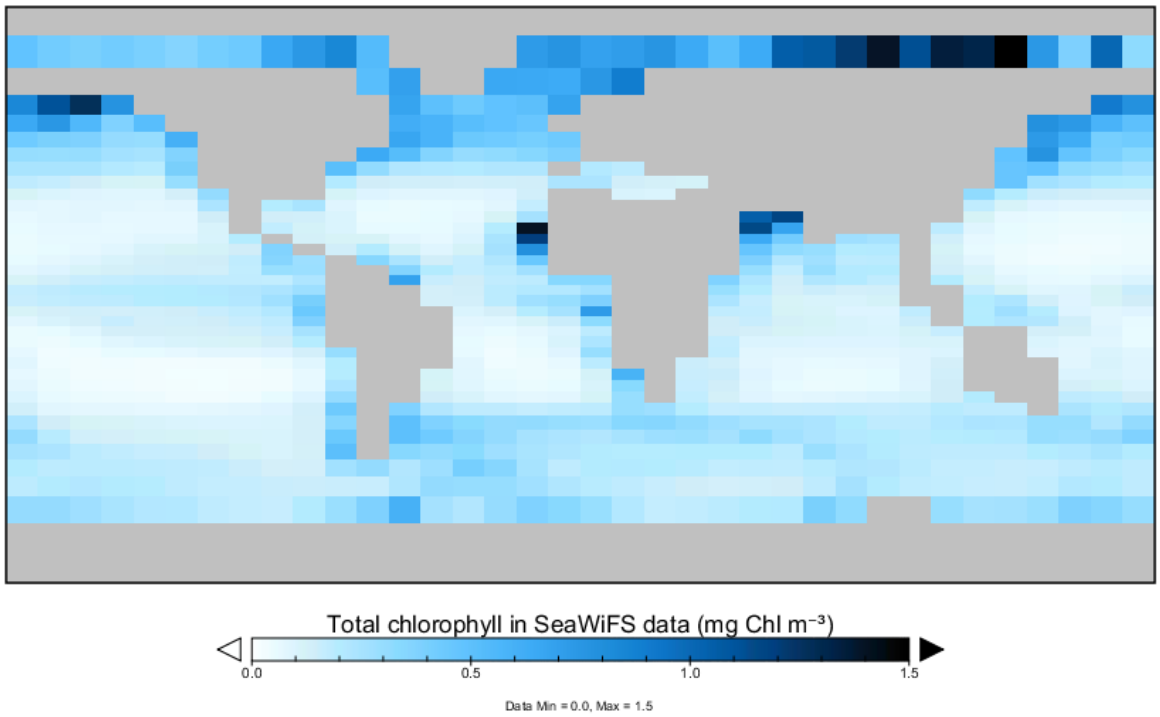

Figure S13: Map illustrating annual mean surface Chlorophyll in SeaWiFS data (climatological average 1997-2002; (NASA Goddard Space Flight Center, 2015)). Plot created with Panoply.

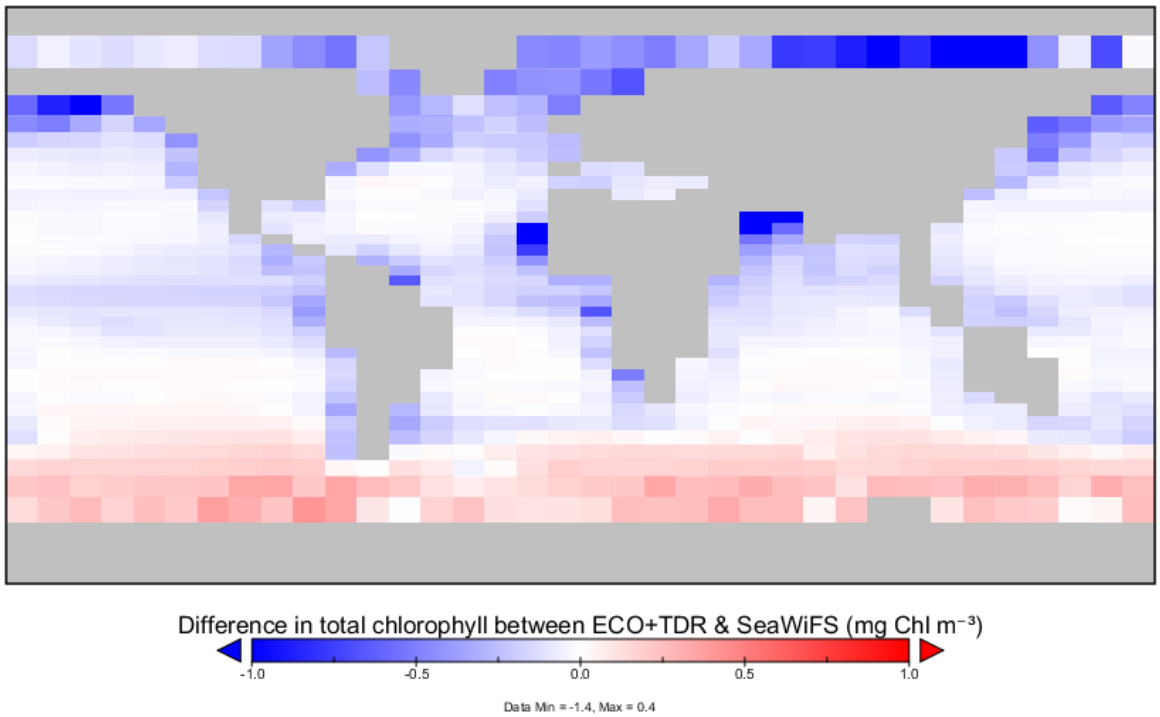

Figure S14: Map illustrating difference in annual mean surface Chlorophyll between our recalibrated ECO+TDR and SeaWiFS data (climatological average 1997-2002; (NASA Goddard Space Flight Center, 2015)). ECO+TDR chlorophyll is in general lower than observed in highly productive coastal regions and higher in the Southern Ocean, but the open ocean is not substantially different relative to the global mean (~0.21 mg Chl m^{-3}). Plot created with Panoply.

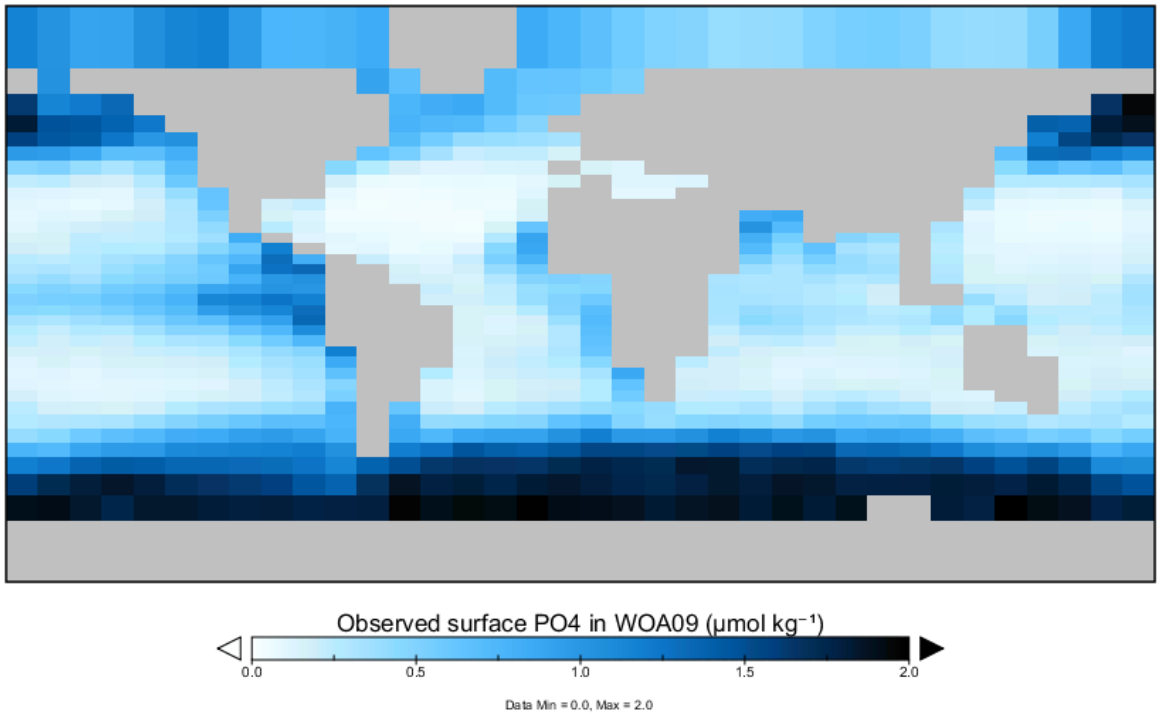

Figure S15: Map illustrating observed surface dissolved phosphate (PO_4) in re-gridded World Ocean Atlas (WOA09) data (Garcia et al., 2010; Ward et al., 2018). Plot created with Panoply.

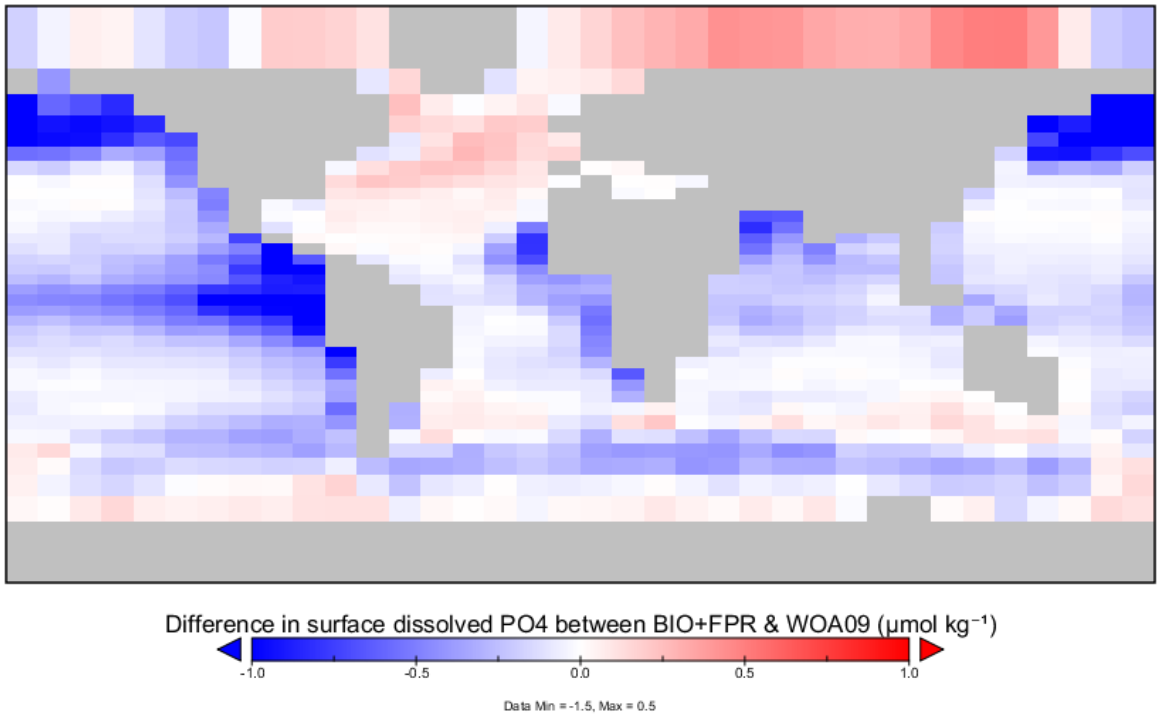

Figure S16: Map illustrating difference in dissolved surface phosphate (PO_4) between BIO+FPR and re-gridded World Ocean Atlas (WOA09) data (Garcia et al., 2010; Ward et al., 2018). BIO+FPR PO_4 is in general less than observed in Pacific-Indian Icean upwelling zones and along the Antarctic Polar Front, but is higher in the North Atlantic and Arctic Ocean., especially in high productivity upwelling regions where PO_4 is ~1 µmol kg^{-1} lower (relative to observed ocean surface mean of ~0.6 µmol kg^{-1}). Plot created with Panoply.

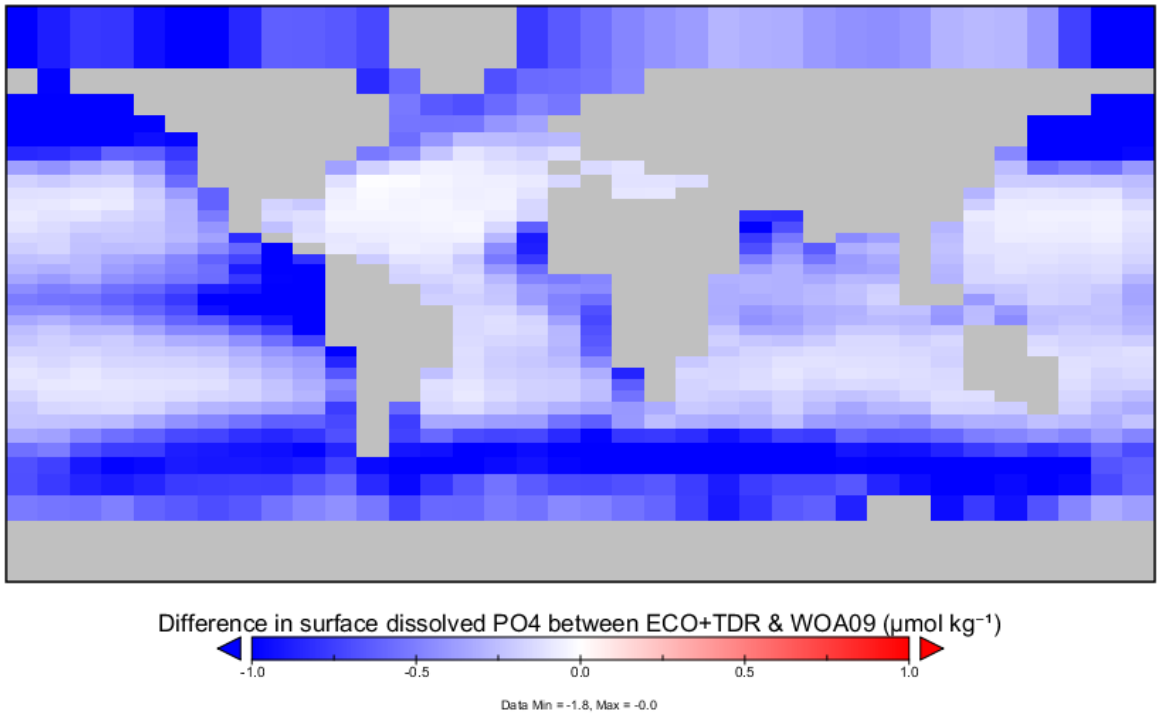

Figure S17: Map illustrating difference in surface PO_4 between our recalibrated ECO+TDR and re-gridded World Ocean Atlas (WOA09) data (Garcia et al., 2010; Ward et al., 2018). ECO+TDR PO_4 is in general less than observed, especially in high productivity upwelling regions where PO_4 is ~1 µmol kg^{-1} lower (relative to observed ocean mean of ~0.6 µmol kg^{-1}). Plot created with Panoply.

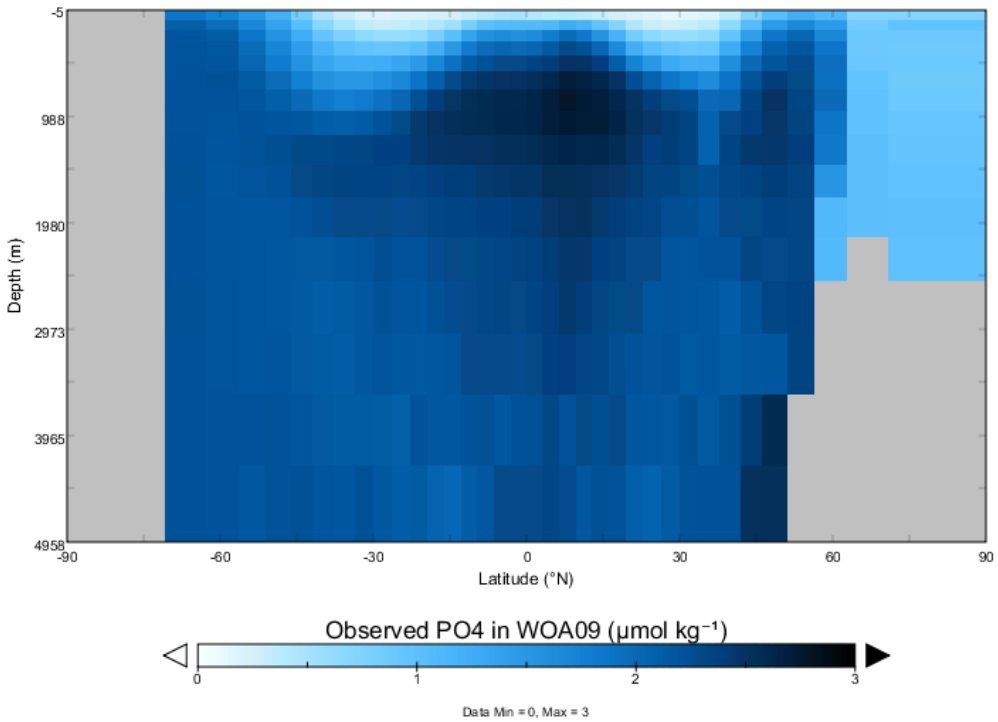

Figure S18: Depth plot illustrating observed dissolved phosphate (PO_4) in re-gridded World Ocean Atlas (WOA09) data (Garcia et al., 2010; Ward et al., 2018). Plot created with Panoply.

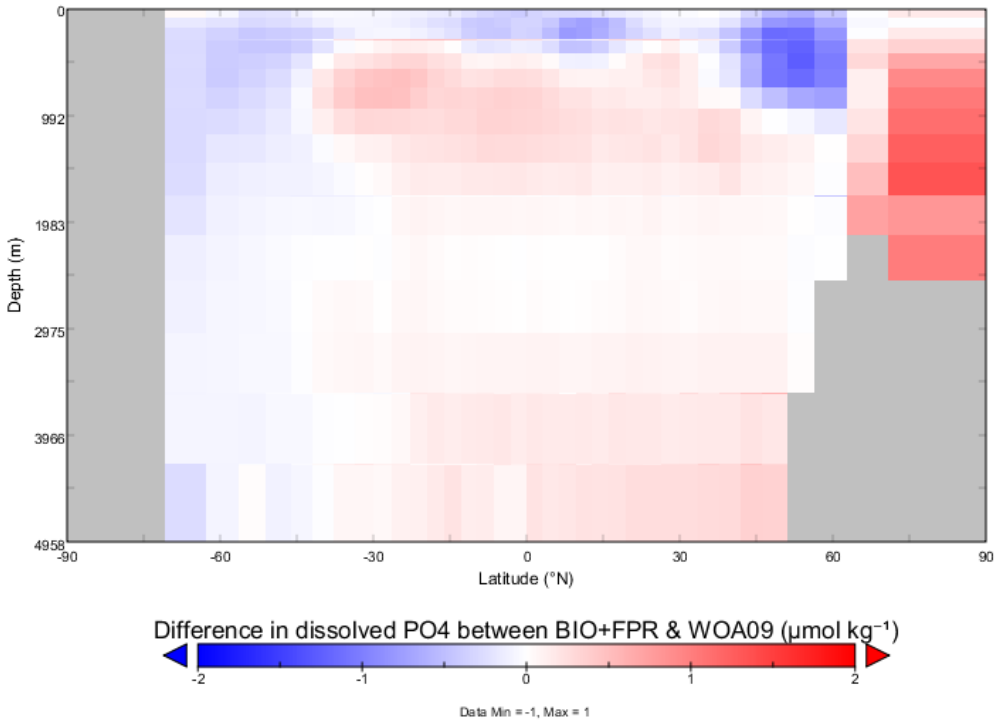

Figure S19: Depth plot illustrating difference in PO_4 between BIO+FPR and re-gridded World Ocean Atlas (WOA09) data (Garcia et al., 2010; Ward et al., 2018). BIO+FPR PO_4 is in general less than observed near the surface and more than observed in low-latitude intermediate and Northern high-latitude deep waters, but the difference is mostly not substantial relative to the observed global mean (~1.7 µmol kg^{-1}). Plot created with Panoply.

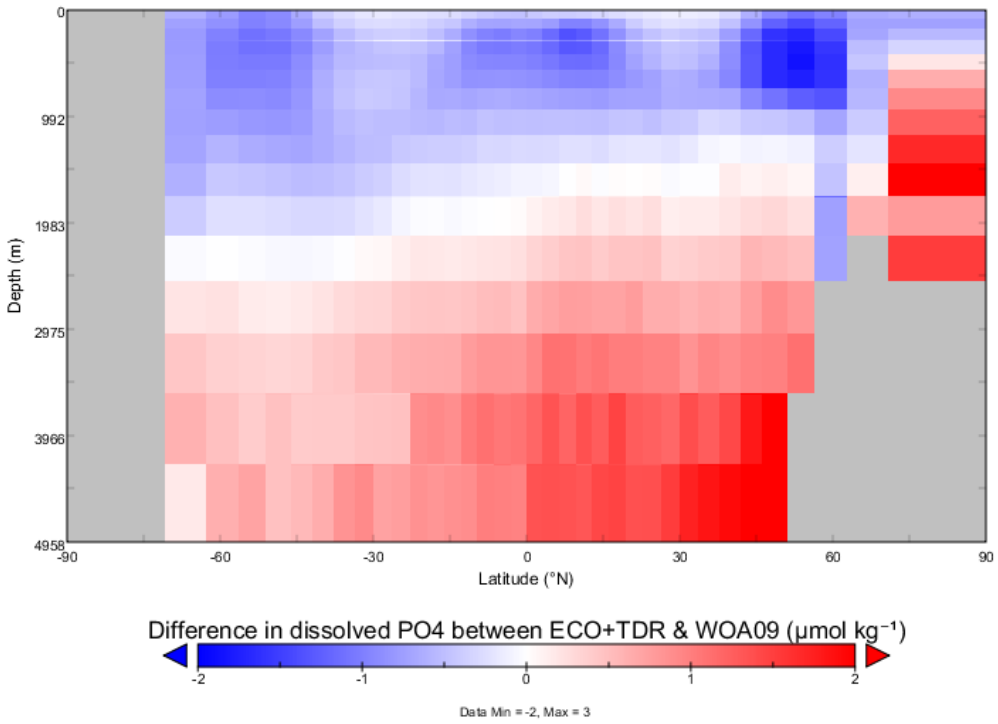

Figure S20: Depth plot illustrating difference in ALK between our recalibrated ECO+TDR and re-gridded World Ocean Atlas (WOA09) data (Garcia et al., 2010; Ward et al., 2018). ECO+TDR PO_4 is in general less than observed in shallow and intermediate depth waters and more than observed in deep and Northern waters. Higher deep water PO_4 relative to BIO+FPR is driven by an elevated POC recalcitrant fraction which is remineralised at the ocean floor. Plot created with Panoply.

3. Recalibrated configurations validation against previous configurations

3.1. DIC in cGEnIE & ecoGEnIE versus previous configurations (Ward et al., 2018)

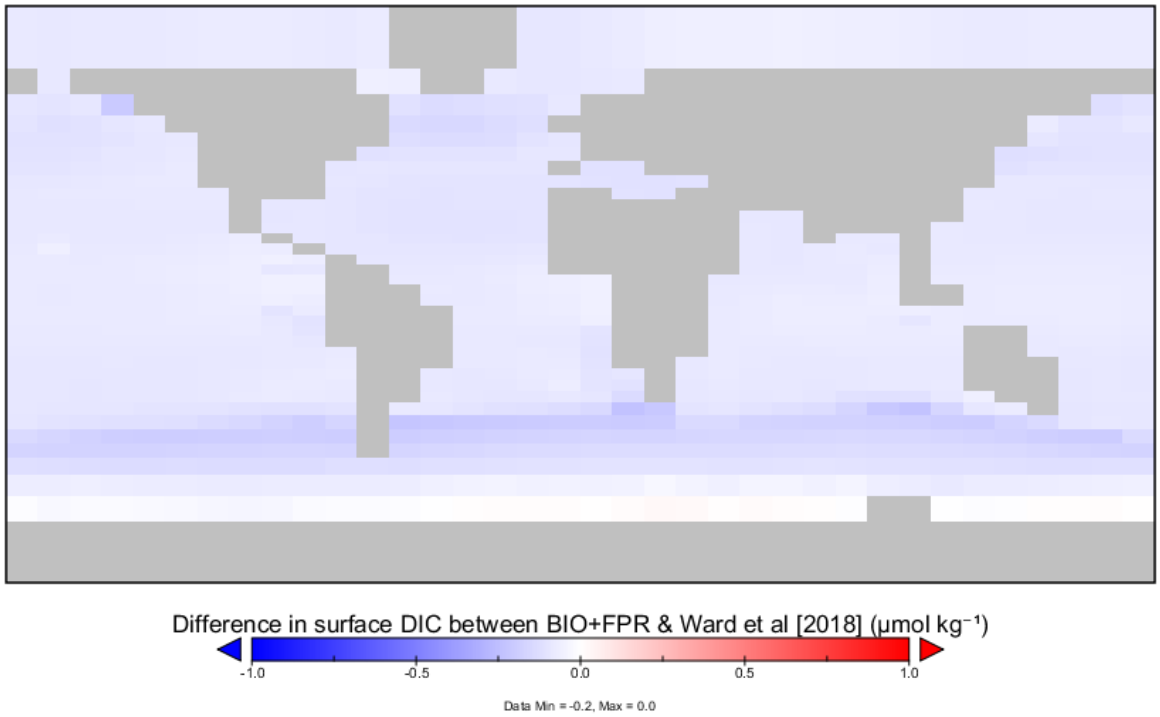

Figure S21: Map illustrating difference in surface DIC BIO+FPR and the default cGEnIE configuration in Ward et al. (2018). BIO+FPR DIC is in general very close to Ward et al. (2018), with variation less than ~0.2 µmol kg^{-1} across the global ocean (relative to a global mean of ~2.3 mmol kg^{-1}). Plot created with Panoply.

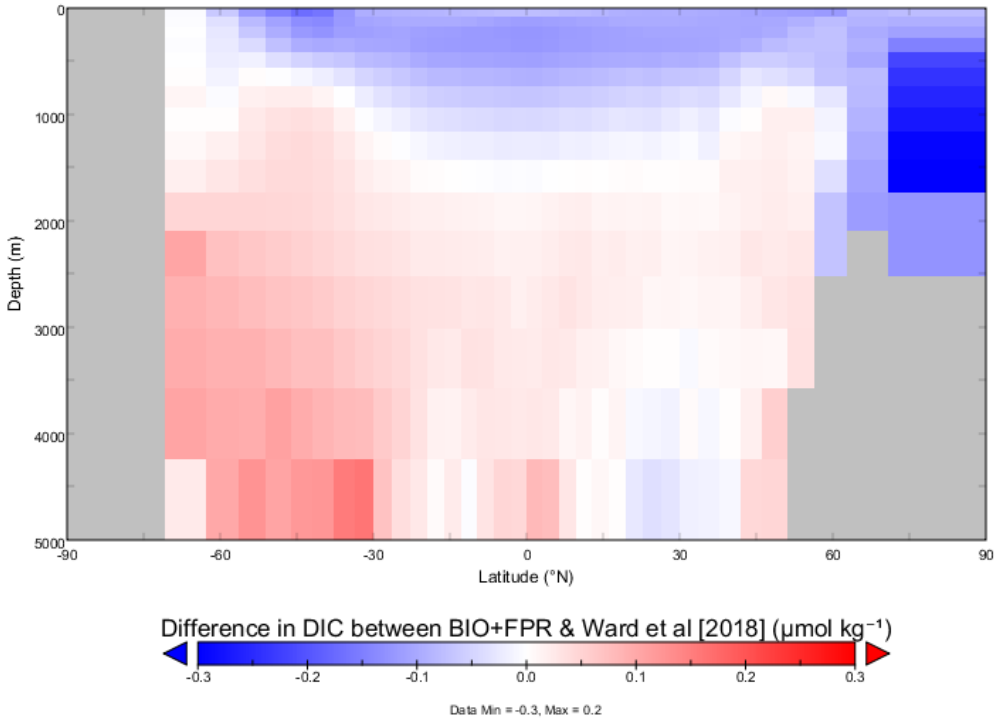

Figure S22: Depth plot illustrating difference in DIC between BIO+FPR and the default cGEnIE configuration in Ward et al. (2018). BIO+FPR DIC is in general very close to Ward et al. (2018), with variation less than ~0.3 µmol kg^{-1} through the global ocean (relative to a global mean of ~2.2 mmol kg^{-1}). Plot created with Panoply.

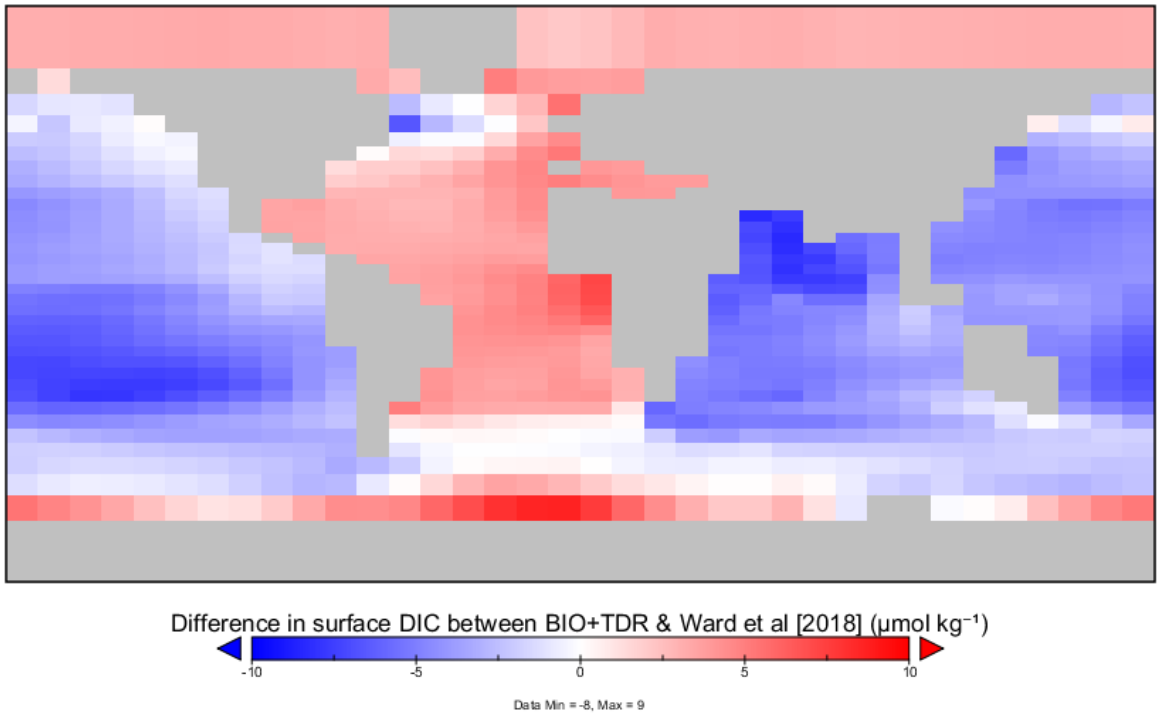

Figure S23: Map illustrating difference in surface DIC between our recalibrated BIO+TDR and the default cGEnIE configuration in Ward et al. (2018). BIO+TDR DIC is in general close to Ward et al. (2018) and the BIO+FPR configuration, with variation less than 10 µmol kg^{-1} across the global ocean (relative to a global mean of ~2 mmol kg^{-1}). Surface DIC is marginally higher in the Atlantic and high-latitudes and lower in the Indian and Pacific Oceans. Plot created with Panoply.

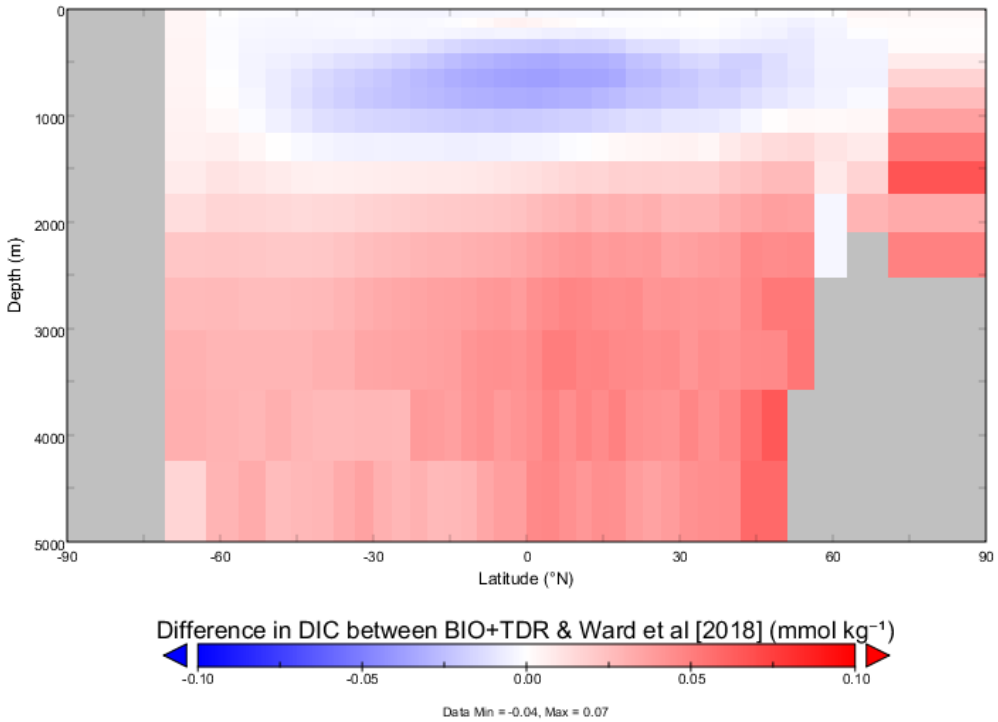

Figure S24: Depth plot illustrating difference in DIC between our recalibrated BIO+TDR and the default cGEnIE configuration in Ward et al. (2018). BIO+TDR DIC is in general close to Ward et al. (2018), with variation less than ~0.1 mmol kg^{-1} through the global ocean (relative to a global mean of ~2.2 mmol kg^{-1}). Plot created with Panoply.

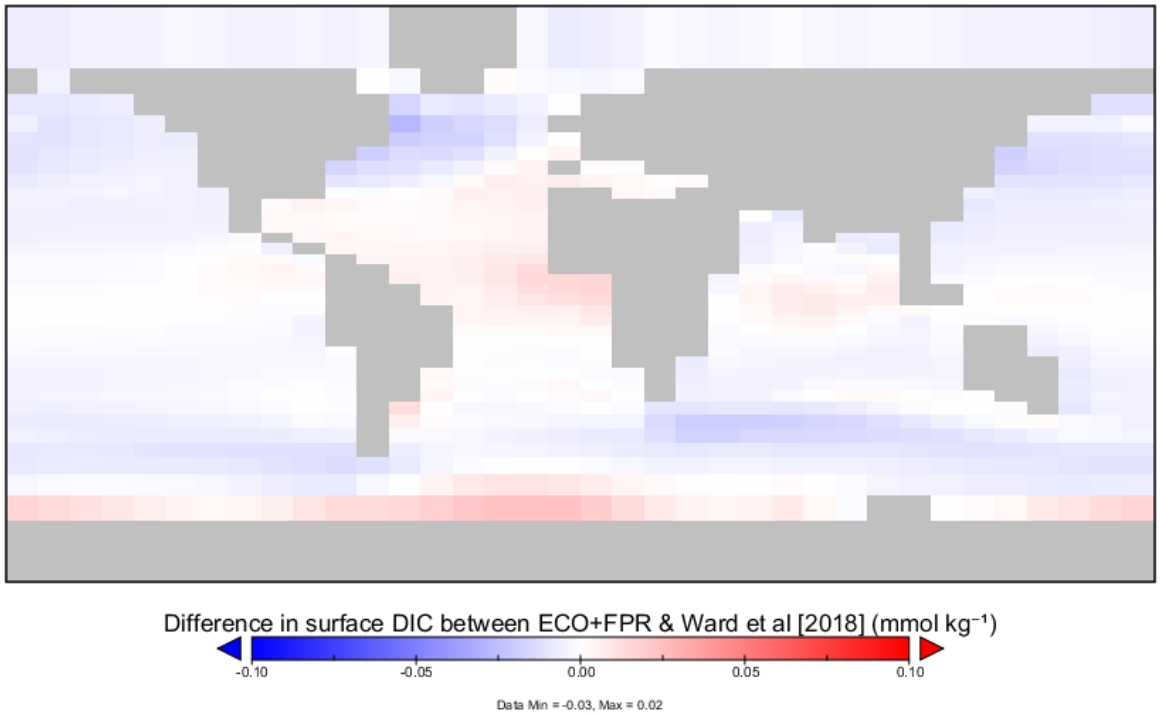

Figure S25: Map illustrating difference in surface DIC between our recalibrated ECO+FPR and the default ecoGEnIE configuration in Ward et al. (2018). ECO+FPR DIC is in general similar to Ward et al. (2018), with variation less than 0.1 mmol kg^{-1} across the global ocean (relative to a global mean of ~2 mmol kg^{-1}). Surface DIC is marginally higher in the Atlantic and Southern Ocean and lower in the Pacific and Arctic Oceans and along the Antarctic Polar Front. Plot created with Panoply.

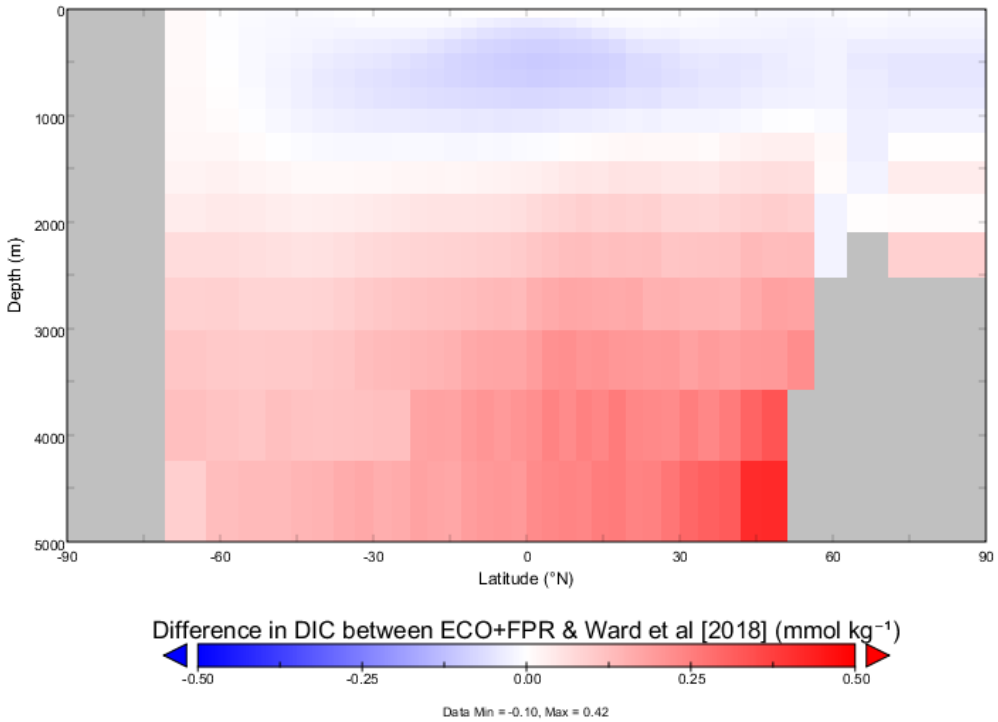

Figure S26: Depth plot illustrating difference in DIC between our recalibrated ECO+FPR and the default ecoGEnIE configuration in Ward et al. (2018). ECO+FPR DIC is in general close to Ward et al. (2018), with variation less than ~0.2 mmol kg^{-1} through most of the global ocean (relative to a global mean of ~2.2 mmol kg^{-1}). The exception is the deep Northern mid-latitudes, as a result of a higher recalcitrant POC fraction from this high productivity region. Plot created with Panoply.

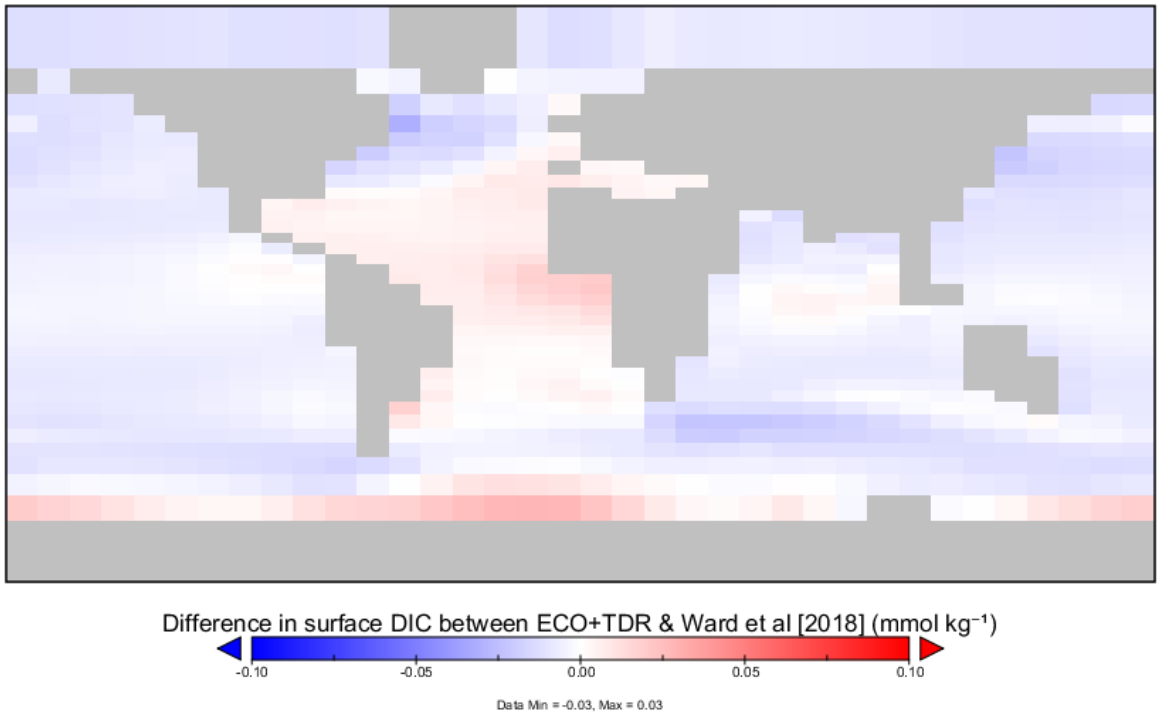

Figure S27: Map illustrating difference in surface DIC between our recalibrated ECO+TDR and the default ecoGEnIE configuration in Ward et al. (2018). ECO+TDR DIC is in general similar to Ward et al. (2018) and to the ECO+FPR configuration, with variation less than 0.1 mmol kg^{-1} across the global ocean (relative to a global mean of ~2 mmol kg^{-1}). Surface DIC is marginally higher in the Atlantic and Southern Ocean and lower in the Indian and Arctic Oceans and along the Antarctic Polar Front. Plot created with Panoply.

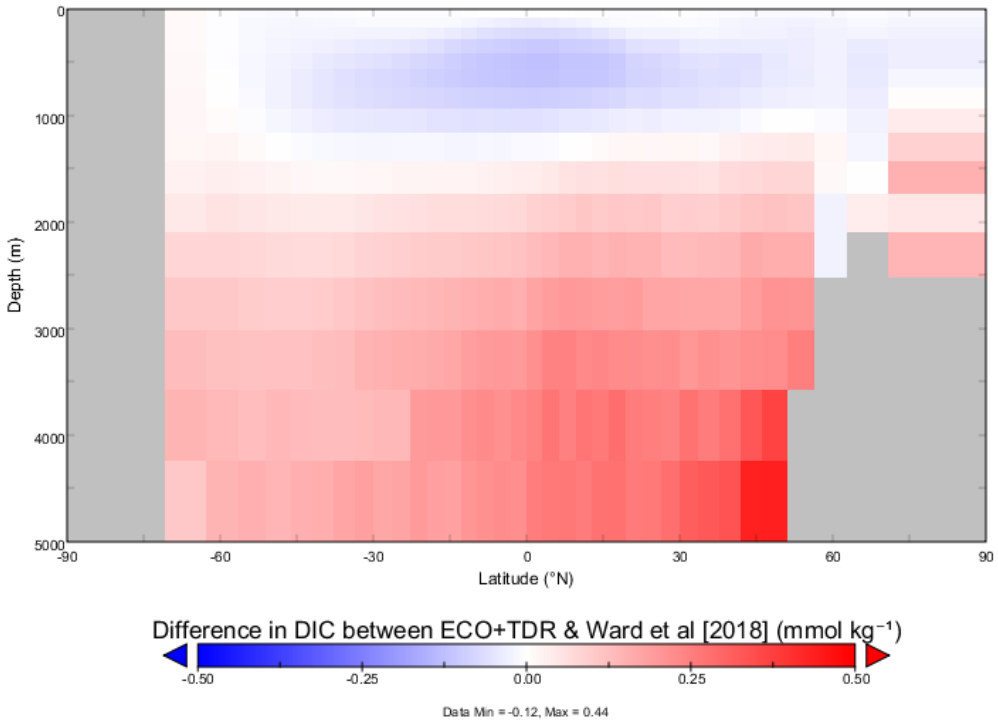

Figure S28: Depth plot illustrating difference in DIC between our recalibrated ECO+TDR and the default ecoGEnIE configuration in Ward et al. (2018). ECO+FPR DIC is in general close to Ward et al. (2018), with variation less than ~0.2 mmol kg^{-1} through most of the global ocean (relative to a global mean of ~2.2 mmol kg^{-1}). The exception is the deep Northern mid-latitudes, as a result of a higher recalcitrant POC fraction from this high productivity region. Plot created with Panoply.

3.2. ALK in cGEnIE & ecoGEnIE versus previous configurations (Ward et al., 2018)

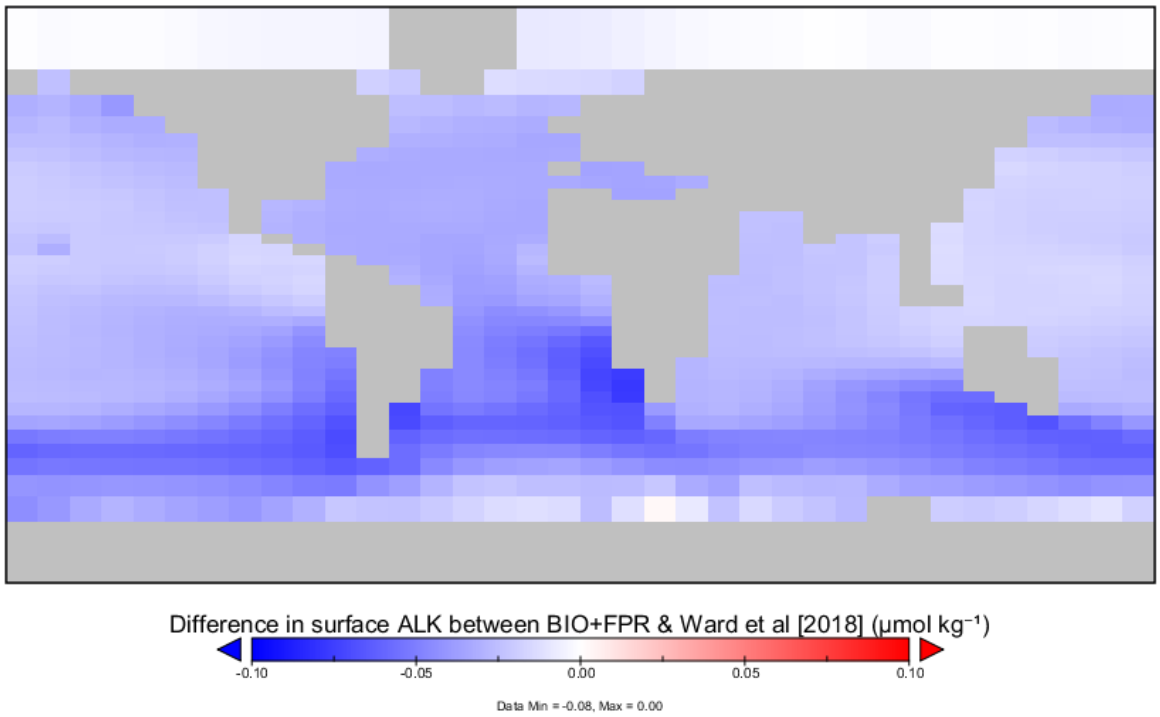

Figure S29: Map illustrating difference in surface ALK between BIO+FPR and the default cGEnIE configuration in Ward et al. (2018). BIO+FPR ALK is in general less than Ward et al. (2018), but the difference is not substantial relative to the global mean (~2.3 mmol kg^{-1}). Plot created with Panoply.

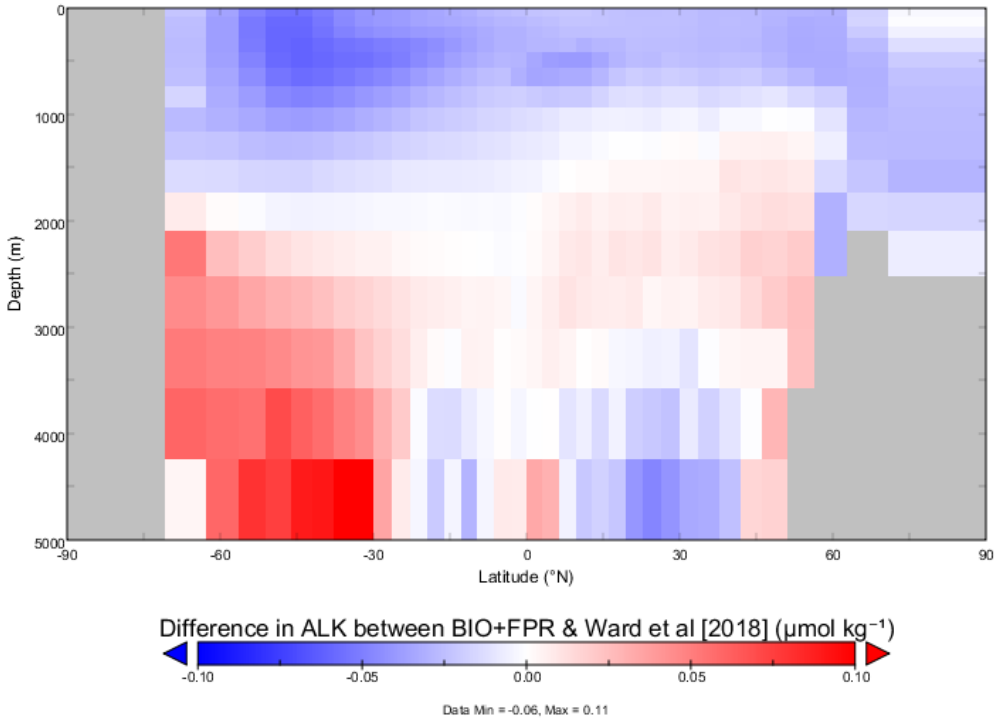

Figure S30: Depth plot illustrating difference in ALK between BIO+FPR and the default cGEnIE configuration in Ward et al. (2018). BIO+FPR ALK is in general less than Ward et al. (2018) in surface and intermediate waters and more in deeper waters, but the difference is not substantial relative to the global mean (up to ~0.1 µmol kg^{-1} versus ~2.3 mmol kg^{-1}). Plot created with Panoply.

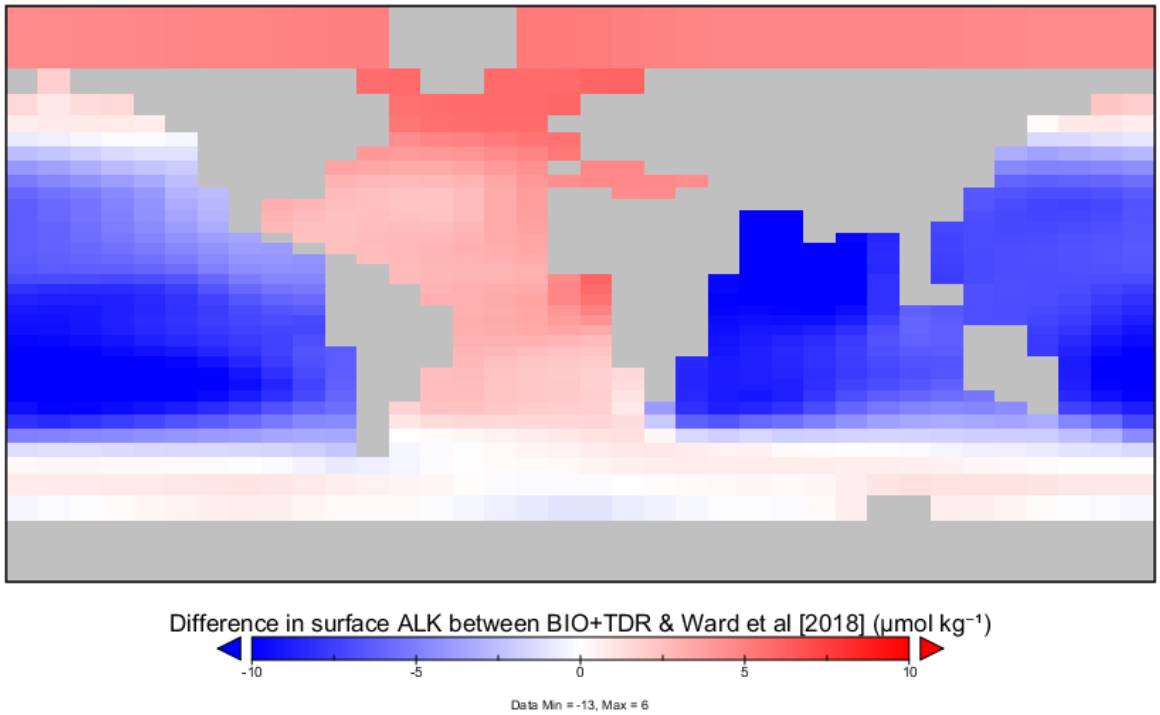

Figure S31: Map illustrating difference in surface ALK between our recalibrated BIO+TDR and the default cGEnIE configuration in Ward et al. (2018). BIO+TDR ALK is in general more in the Atlantic and Arctic Oceans and less in the Indian and Pacific Oceans than Ward et al. (2018) as a result of prioritising tuning for optimal DIC speciation, but the difference is not substantial relative to the global mean (~2.3 mmol kg^{-1}). Plot created with Panoply.

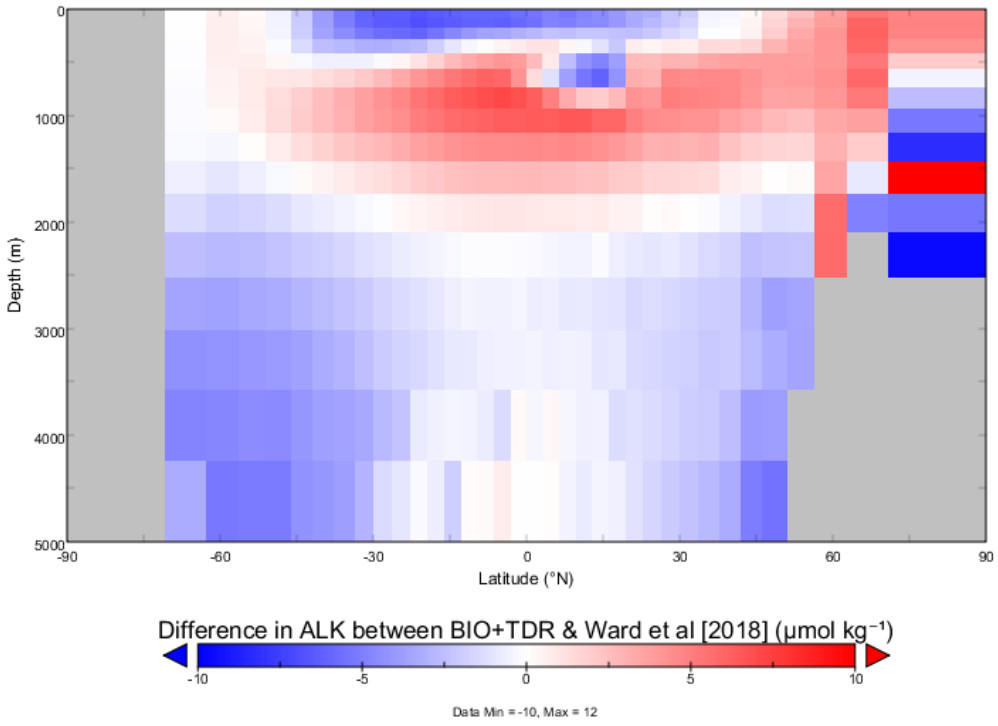

Figure S32: Depth plot illustrating difference in ALK between our recalibrated BIO+TDR and the default cGEnIE configuration in Ward et al. (2018). BIO+TDR ALK is in general less than Ward et al. (2018) in surface low-latitude and deep waters and more in intermediate and surface high-latitude waters, but the difference is not substantial relative to the global mean (up to ~10 µmol kg^{-1} versus ~2.3 mmol kg^{-1}). Plot created with Panoply.

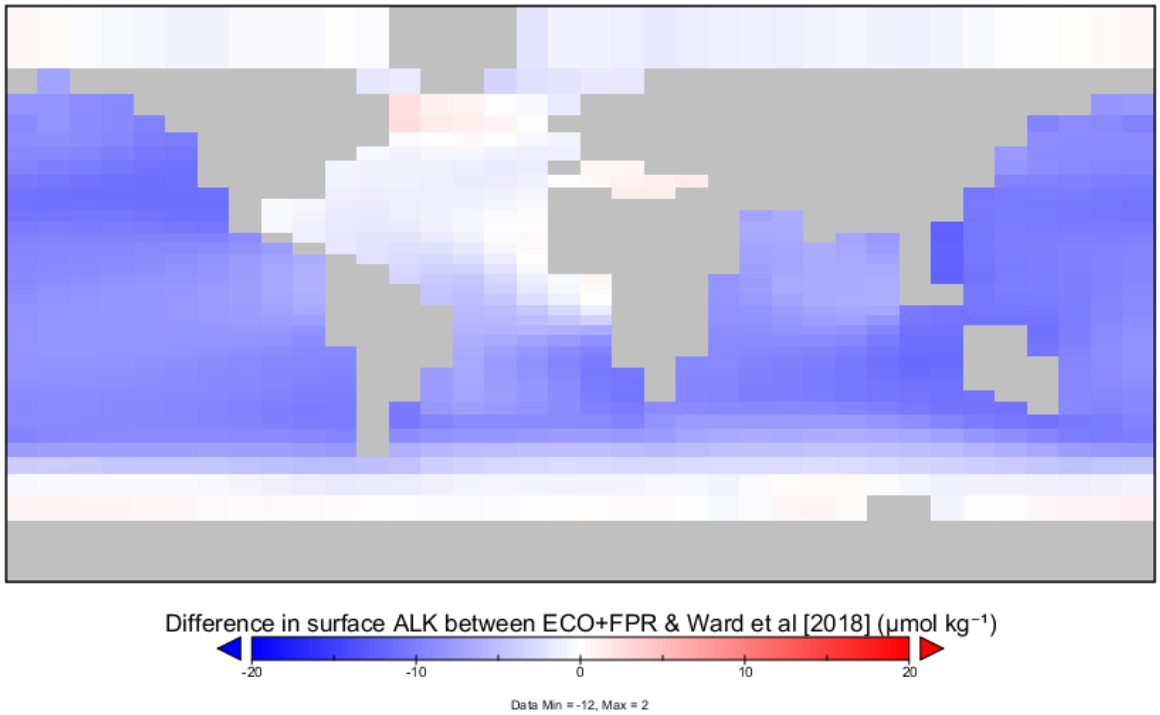

Figure S33: Map illustrating difference in surface ALK between our recalibrated ECO+FPR and the default ecoGEnIE configuration in Ward et al. (2018). ECO+FPR ALK is in general similar to Ward et al. (2018) with marginally lower values apparent in the Indian and Pacific Oceans, but the difference is not substantial relative to the global mean (~2.3 mmol kg^{-1}). Plot created with Panoply.

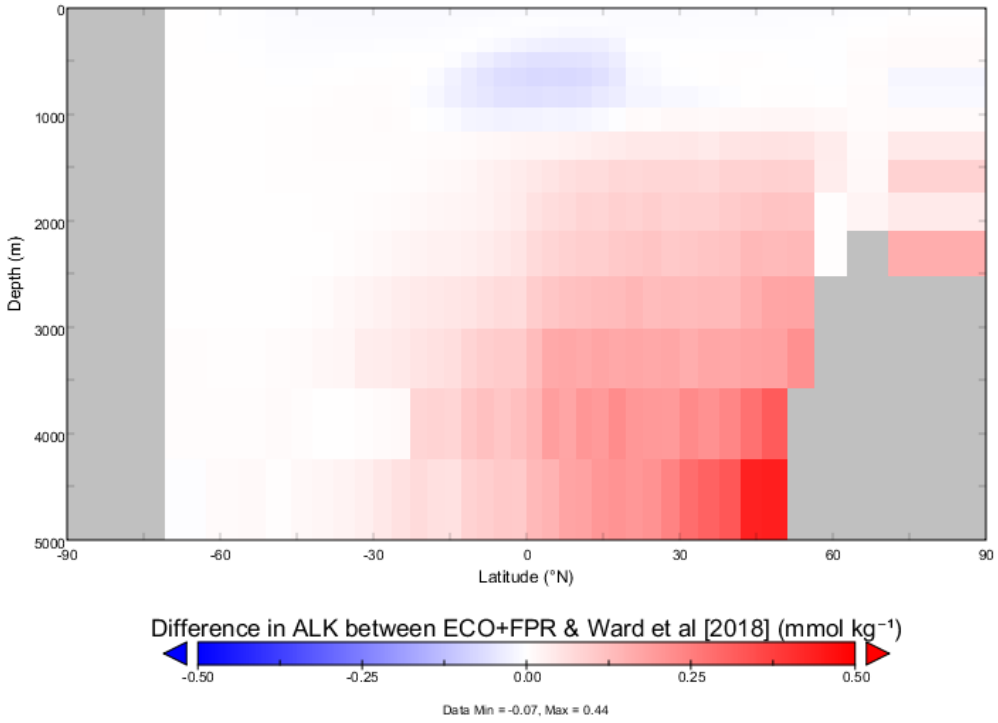

Figure S34: Depth plot illustrating difference in ALK between our recalibrated ECO+FPR and the default ecoGEnIE configuration in Ward et al. (2018). ECO+FPR ALK is in general similar to Ward et al. (2018) but slightly higher values in deep Northern waters, but the difference is not substantial relative to the global mean (up to ~0.5 mmol kg^{-1} versus ~2.3 mmol kg^{-1}). Plot created with Panoply.

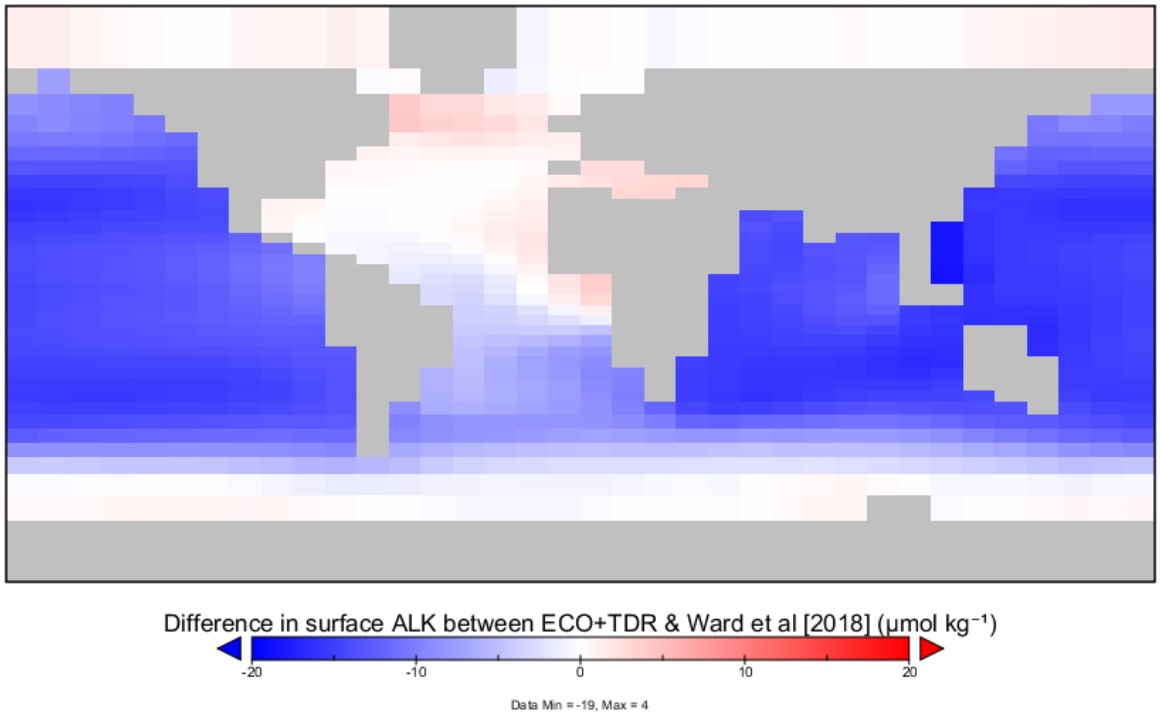

Figure S35: Map illustrating difference in surface ALK between our recalibrated ECO+TDR and the default ecoGEnIE configuration in Ward et al. (2018). ECO+TDR ALK is in general similar to Ward et al. (2018) and to the ECO+FPR configuration with marginally lower values apparent in the Indian and Pacific Oceans, but the difference is not substantial relative to the global mean (~2.3 mmol kg^{-1}). Plot created with Panoply.

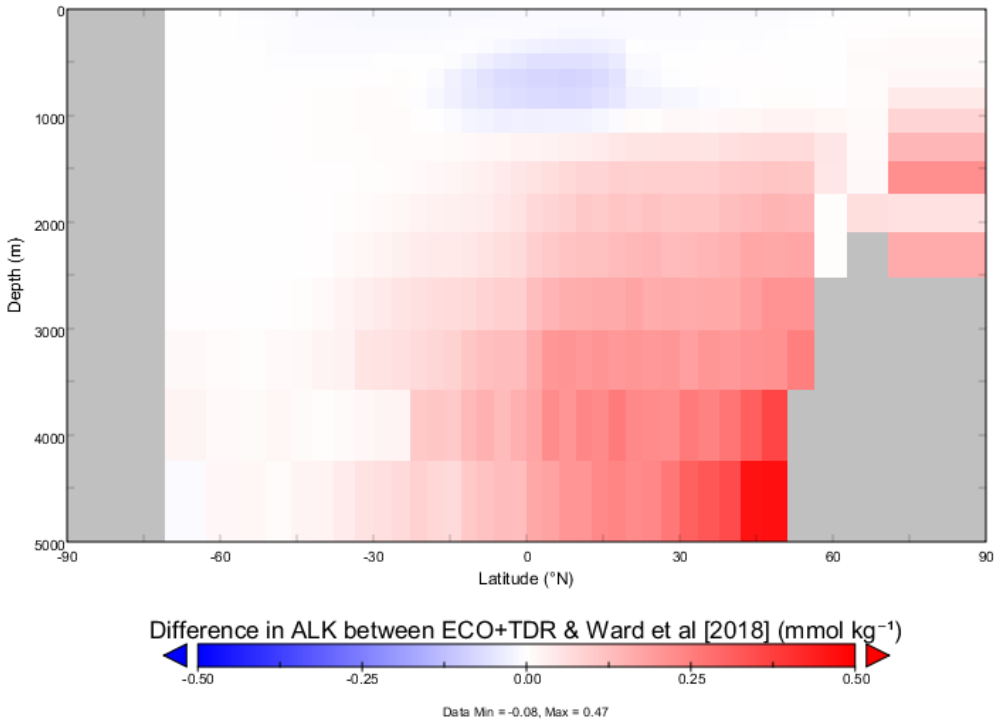

Figure S36: Depth plot illustrating difference in ALK between o recalibrated ECO+TDR and the default ecoGEnIE configuration in Ward et al. (2018). ECO+TDR ALK is in general similar to Ward et al. (2018) with slightly higher values in deep Northern waters, but the difference is not substantial relative to the global mean (up to ~0.5 mmol kg^{-1} versus ~2.3 mmol kg^{-1}). Plot created with Panoply.

3.3. *PO_4 in cGEnIE & ecoGEnIE versus previous configurations (Ward et al., 2018)*

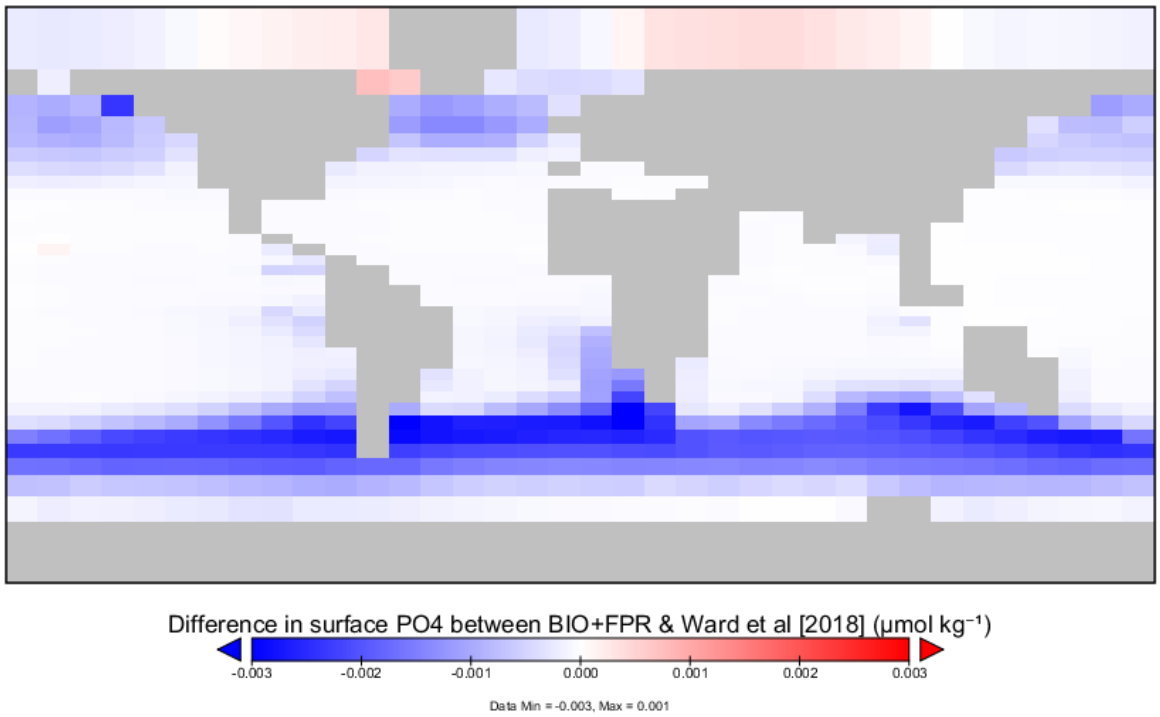

Figure S37: Map illustrating difference in surface PO_4 between BIO+FPR and the default cGEnIE configuration in Ward et al. (2018). BIO+FPR cGEnIE PO_4 is in general very similar to Ward et al. (2018) (with differences less than ~0.003 µmol kg^{-1} relative to observed ocean surface mean of ~0.6 µmol kg^{-1}). Plot created with Panoply.

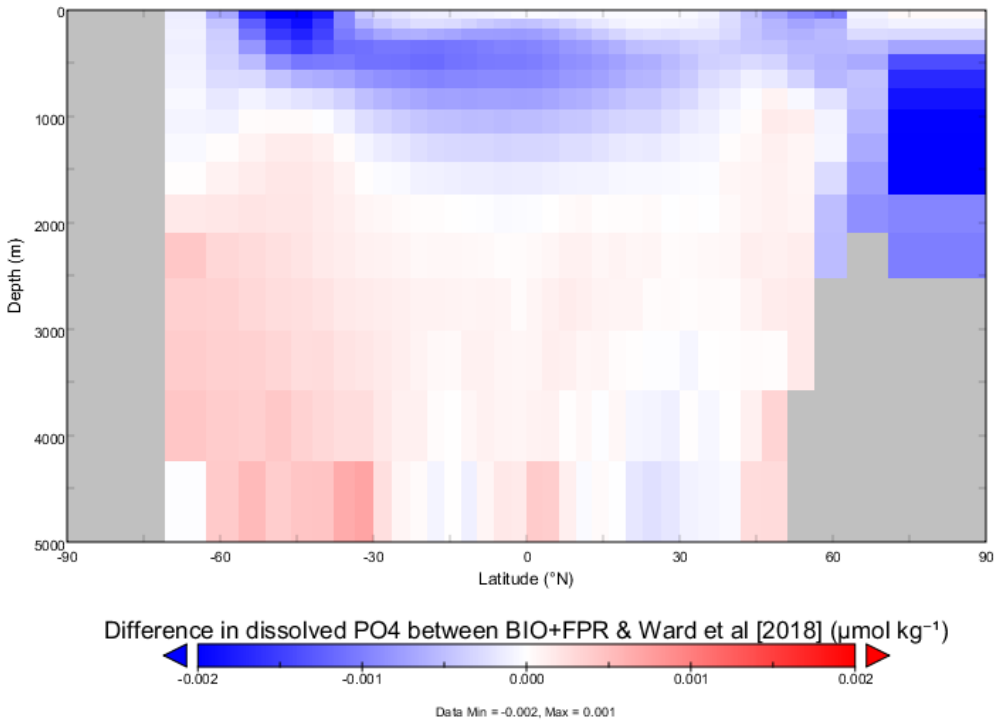

Figure S38: Depth plot illustrating difference in surface PO_4 between BIO+FPR and the default cGEnIE configuration in Ward et al. (2018). BIO+FPR cGEnIE PO_4 is in general very similar to Ward et al. (2018) (with differences less than ~0.002 µmol kg^{-1} relative to observed ocean mean of ~1.8 µmol kg^{-1}), with slightly lower values towards the surface and slightly higher values in deep waters. Plot created with Panoply.

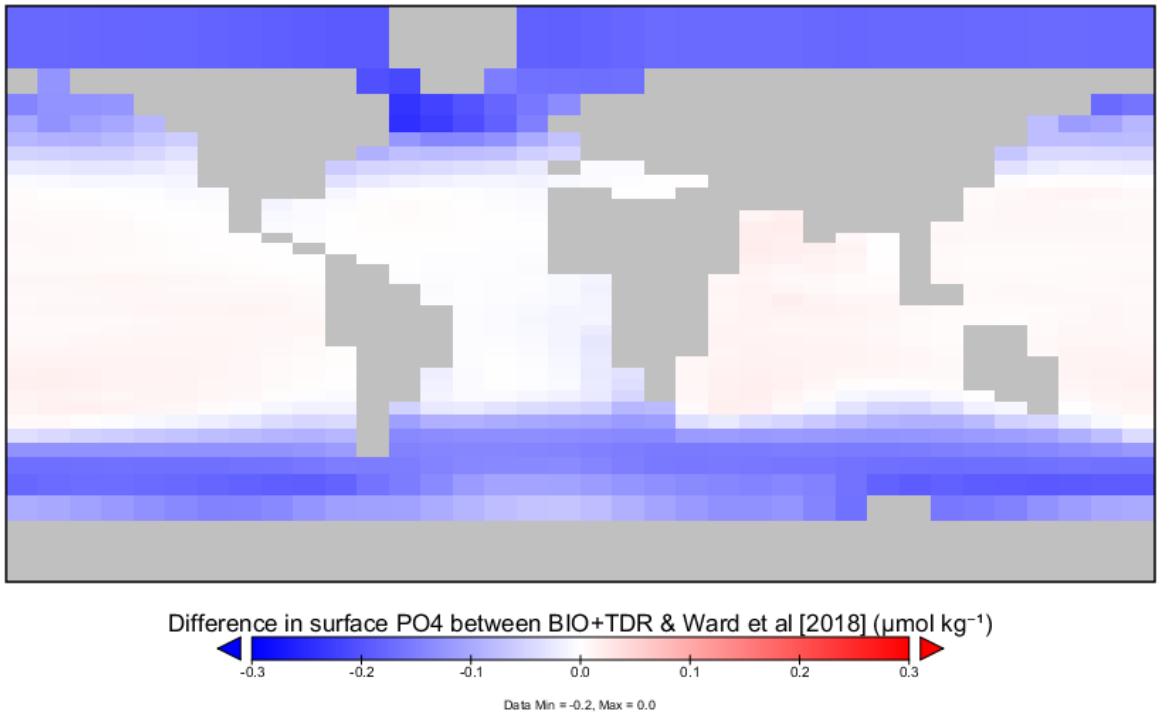

Figure S39: Map illustrating difference in surface PO_4 between our recalibrated BIO+TDR and the default cGEnIE configuration in Ward et al. (2018). BIO+TDR PO_4 is in general similar to Ward et al. (2018) in low-latitude waters but reaches ~0.2 µmol kg^{-1} less in some higher latitude regions (relative to observed ocean surface mean of ~0.6 µmol kg^{-1}). Plot created with Panoply.

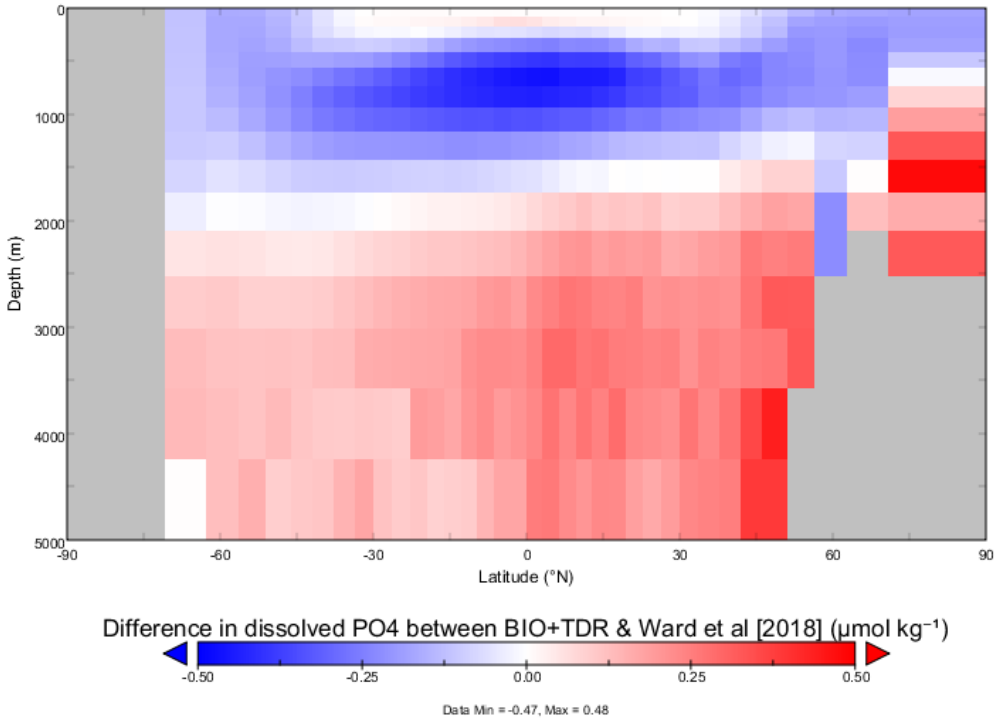

Figure S40: Depth plot illustrating difference in surface PO_4 between our recalibrated BIO+TDR and the default cGEnIE configuration in Ward et al. (2018). BIO+TDR PO_4 in general has lower values in intermediate waters and higher values in deeper waters and just below the surface compared with Ward et al. (2018) (with differences up to ~0.5 µmol kg^{-1} relative to observed ocean mean of ~1.8 µmol kg^{-1}). This reflects higher nutrient recycling due to temperature-dependent remineralisation near the surface reducing nutrient supply to intermediate waters, and in deeper waters higher values reflect a higher recalcitrant POC fraction remineralised at the ocean floor. Plot created with Panoply.

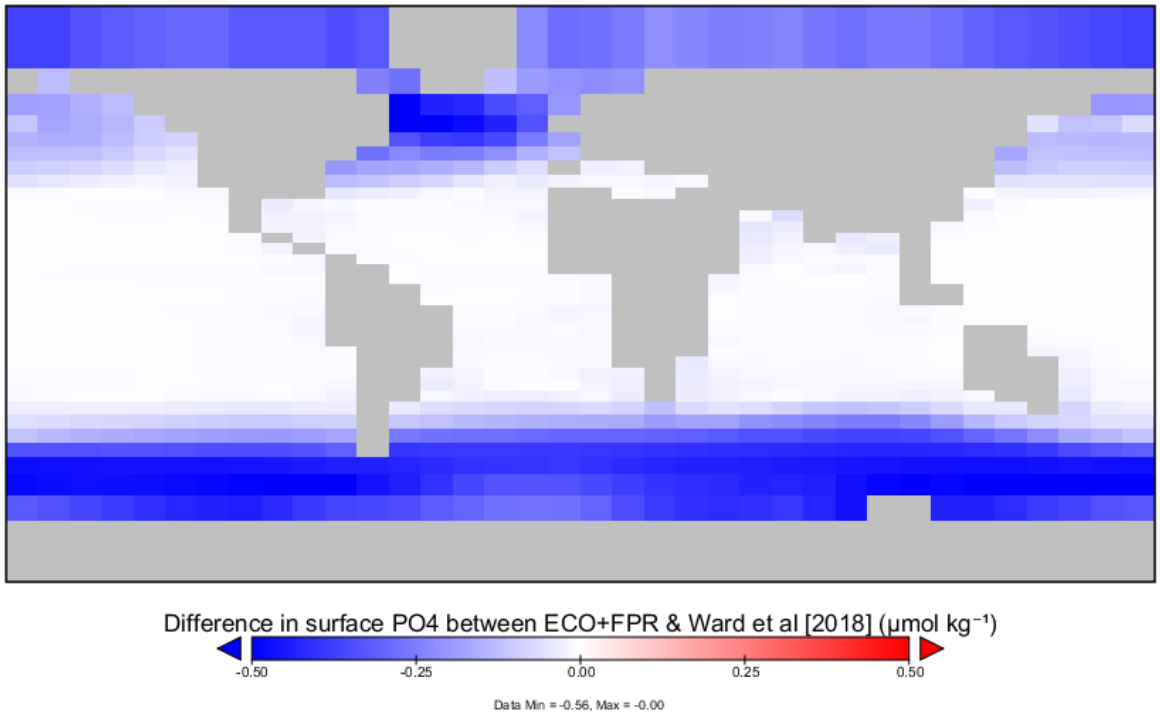

Figure S41: Map illustrating difference in surface PO_4 between our recalibrated ECO+FPR and the default ecoGEnIE configuration in Ward et al. (2018). ECO+FPR PO_4 is in general similar to Ward et al. (2018) in subpolar waters, with greater differences apparent in higher latitudes and the North Atlantic (up to ~0.5 µmol kg^{-1} relative to observed ocean surface mean of ~0.6 µmol kg^{-1}). This reflects greater production and export in higher latitudes and reduced nutrient flux to the North Atlantic in ECO+FPR. Plot created with Panoply.

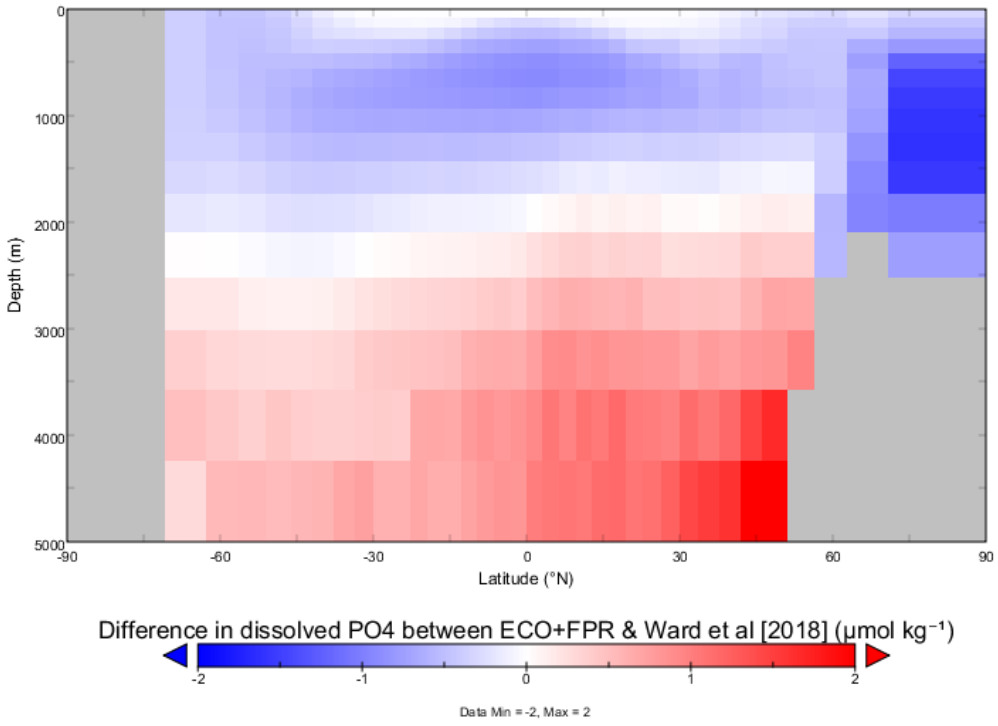

Figure S42: Depth plot illustrating difference in surface PO_4 between our recalibrated ECO+FPR and the default ecoGEnIE configuration in Ward et al. (2018). ECO+FPR PO_4 in general has lower values in intermediate waters and higher values in deeper waters compared with Ward et al. (2018) (with differences up to ~0.5 µmol kg^{-1} in most of the ocean relative to observed ocean mean of ~1.8 µmol kg^{-1}, but values up to 2 µmol kg^{-1} higher in deep Northern waters). This reflects a higher recalcitrant POC fraction in this configuration being remineralised at the ocean floor. Plot created with Panoply.

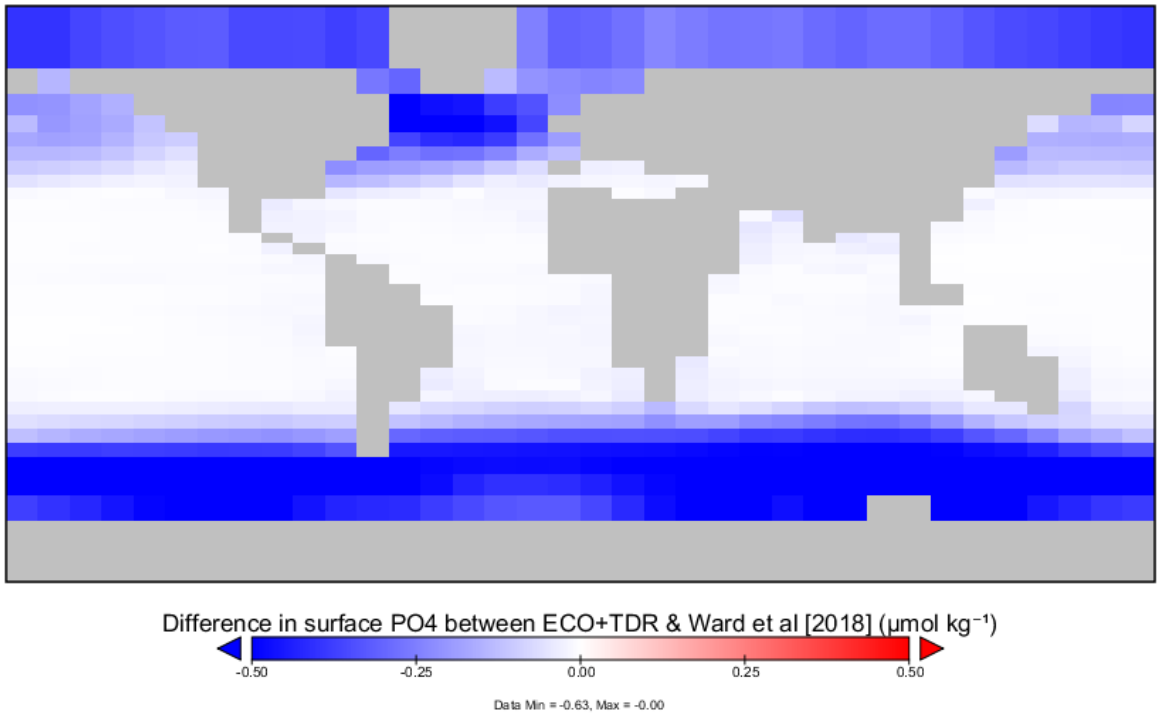

Figure S43: Map illustrating difference in surface PO_4 between our recalibrated ECO+TDR and the default ecoGEnIE configuration in Ward et al. (2018). ECO+TDR PO_4 is in general similar to Ward et al. (2018) in lower latitude waters and very similar to the ECO+FPR configuration, with greater differences apparent in higher latitudes and the North Atlantic (up to ~0.5 µmol kg^{-1} relative to observed ocean surface mean of ~0.6 µmol kg^{-1}). This reflects greater production and export in higher latitudes and reduced nutrient flux to the North Atlantic in ECO+TDR. Plot created with Panoply.

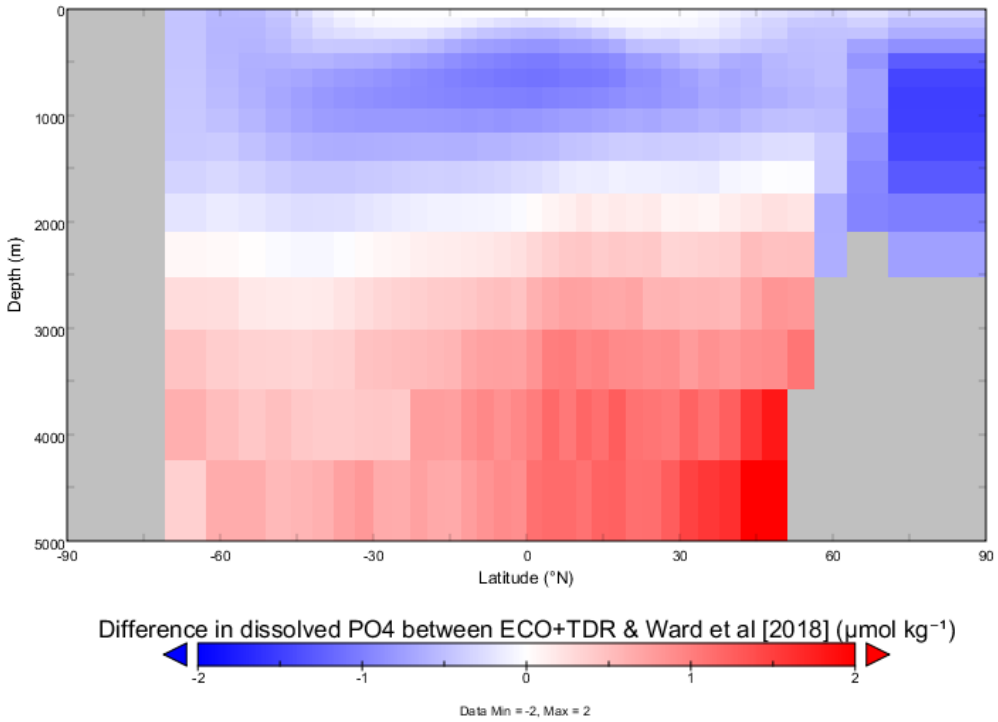

Figure S44: Depth plot illustrating difference in surface PO_4 between our recalibrated ECO+TDR and the default ecoGEnIE configuration in Ward et al. (2018). ECO+TDR PO_4 in general has lower values in intermediate waters and higher values in deeper waters compared with Ward et al. (2018) (with differences up to ~1 µmol kg^{-1} relative to observed ocean mean of ~1.8 µmol kg^{-1}, but values up to 2 µmol kg^{-1} higher in deep Northern waters). This reflects higher nutrient recycling due to temperature-dependent remineralisation near the surface reducing nutrient supply to intermediate waters, and in deeper waters higher values reflect a higher

recalcitrant POC fraction remineralised at the ocean floor. Plot created with Panoply.

3.4. Aragonite saturation state (Ω) comparison between ECO+TDR and BIO+FPR

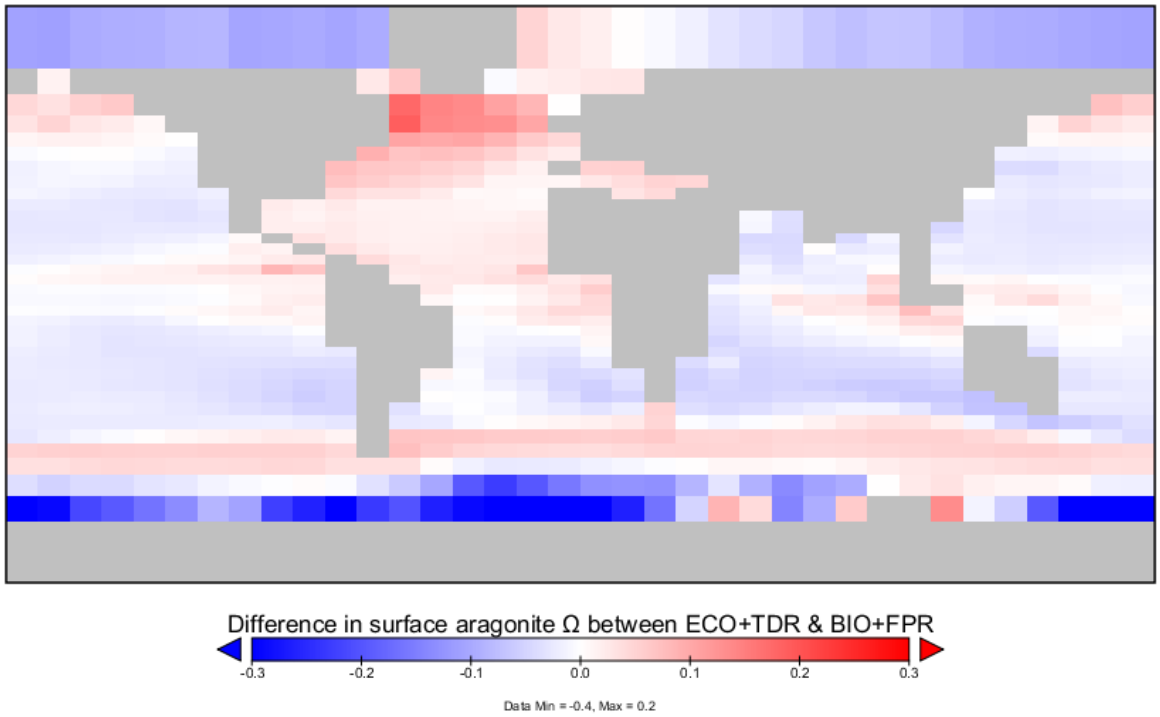

Figure S45: Map illustrating difference in preindustrial surface aragonite saturation state (Ω) between our recalibrated ECO+TDR and BIO+FPR. ECO+TDR Ω is in general slightly higher in the North Atlantic and productive upwelling regions and lower in oligotrophic and especially polar regions than BIO+FPR, but the difference is not substantial relative to the global mean (~2.9). Plot created with Panoply.

4. Supplementary Results Figures

4.1. Physical Climate Response

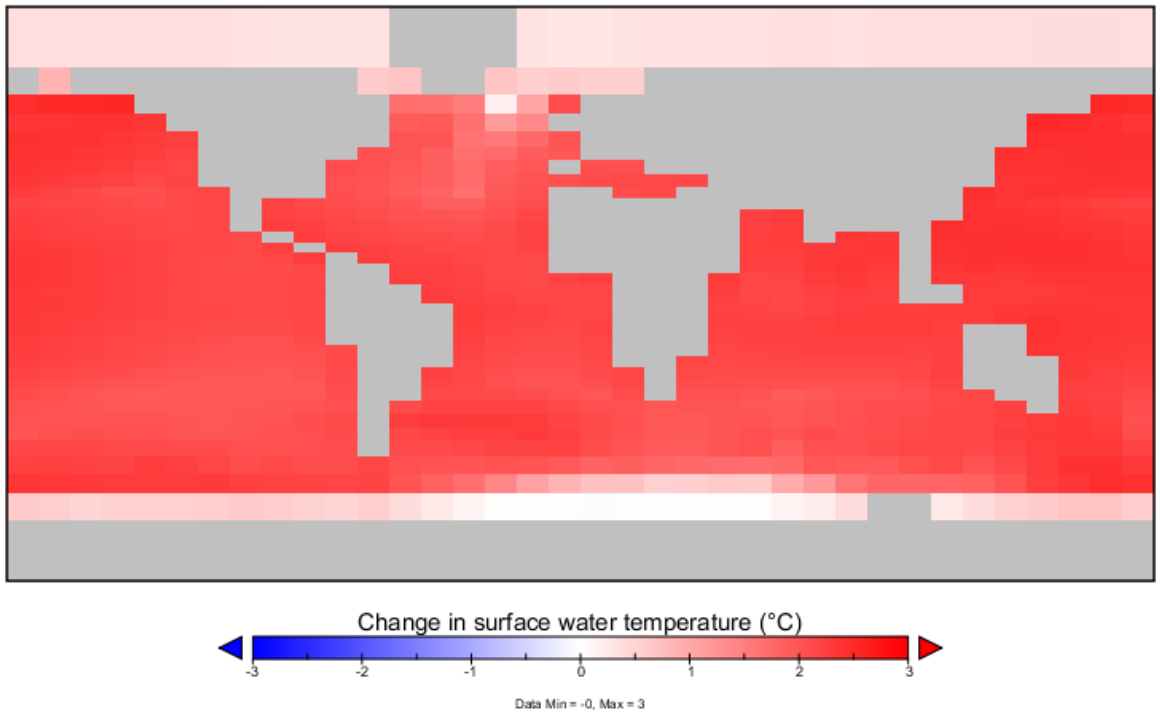

Figure S46: Map illustrating the change in surface water temperature by 2100 CE under RCP4.5 (BIO+FPR), showing spatial warming patterns. Warming mostly occurs in low and mid-latitude waters, except for in the North Atlantic as a result of a slowdown in Atlantic meridional overturning circulation. Plot created with Panoply.

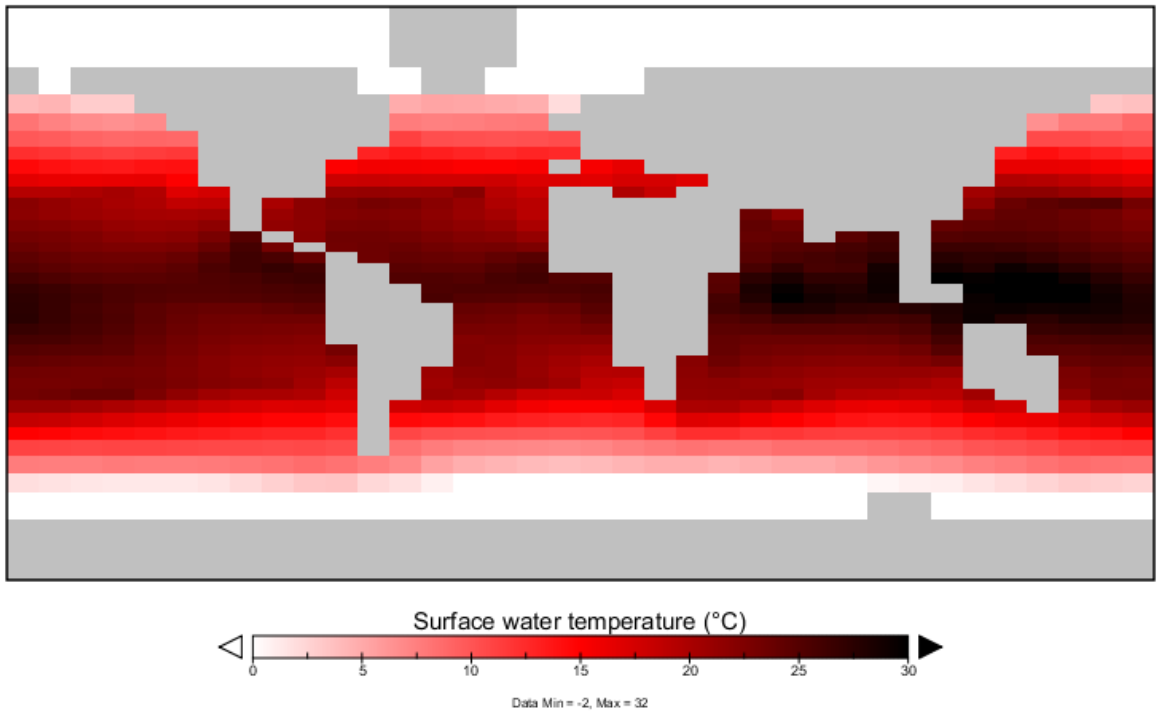

Figure S47: Map illustrating preindustrial surface water temperature in BIO+FPR, showing pre-warming spatial temperature patterns. Plot created with Panoply.

4.2. *Biological Pump Strength*

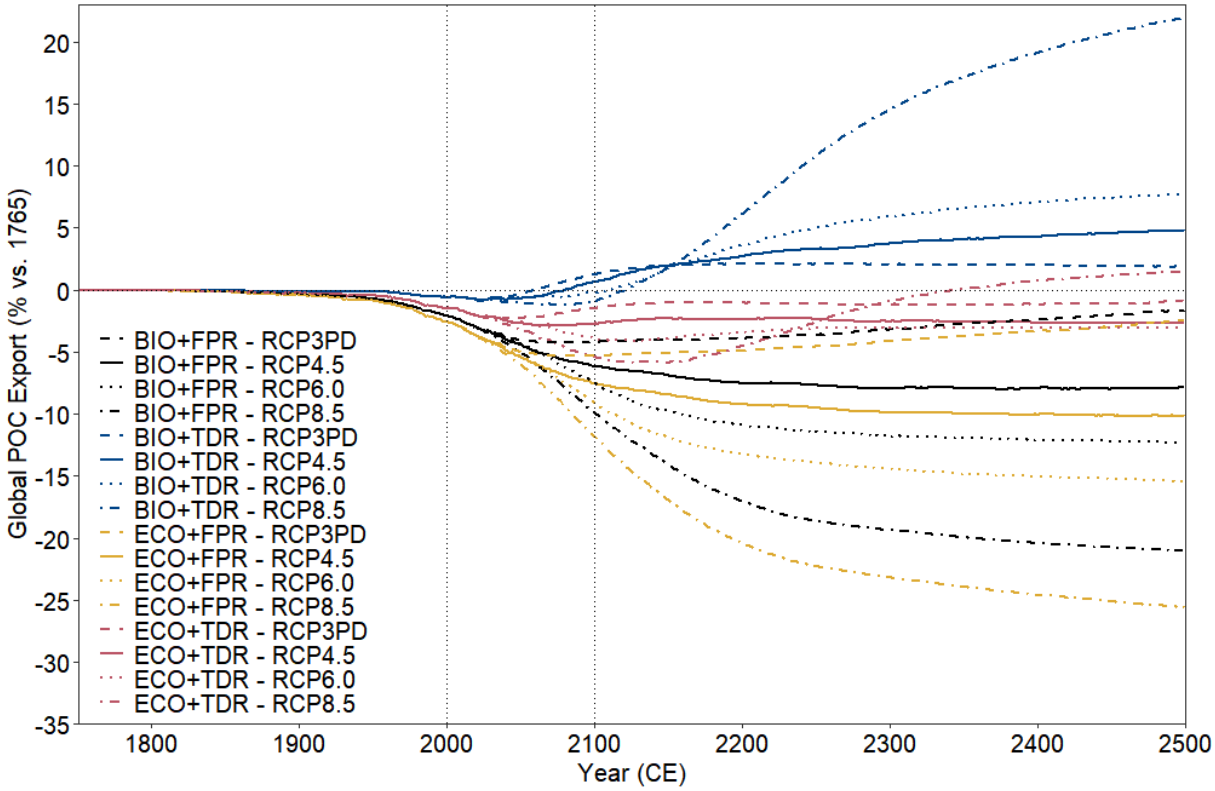

Figure S48: cGEnIE/ecoGEnIE simulation results for global POC export flux under different configurations and forcing scenarios. Results for RCPs 3PD (dashed lines), 4.5 (solid lines), 6.0 (dotted lines) and 8.5 (dot-dashed lines) are shown for each of the default calibration configurations (BIO+FPR – black; BIO+TDR – blue; ECO+FPR – yellow; ECO+TDR – red), and the baseline POC export and the 21st century (used for cumulative POC flux and ocean carbon sink capacity calculations in Table 2) marked by the horizontal and vertical dotted lines respectively.

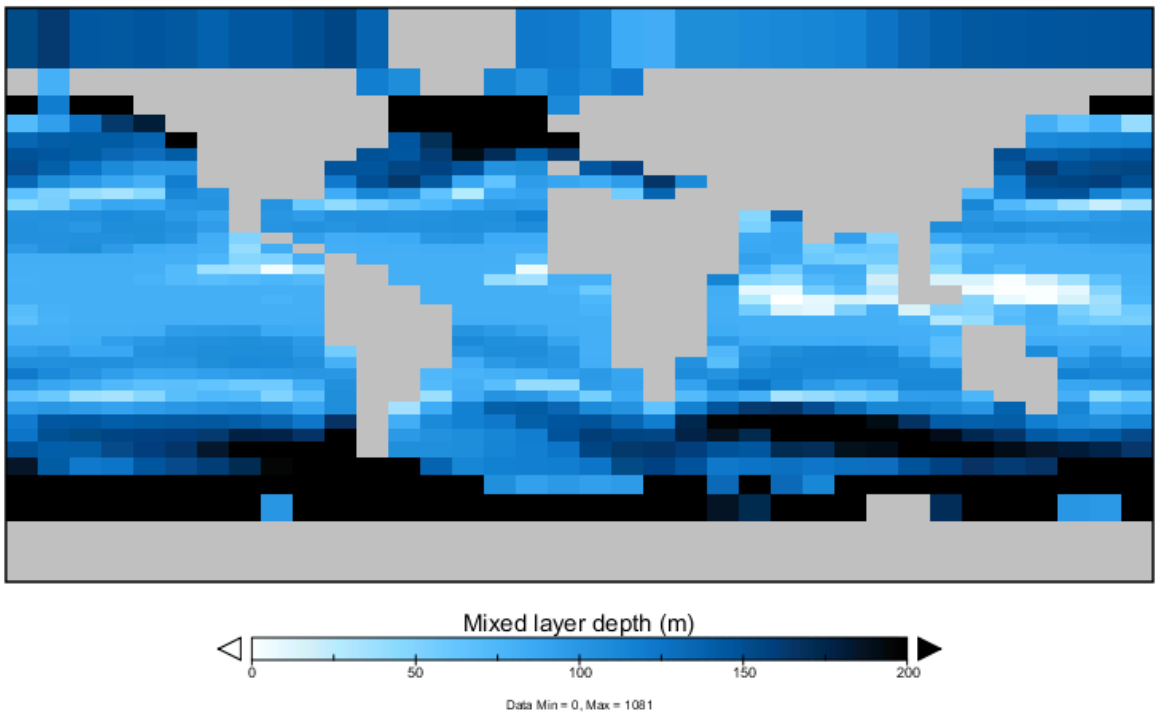

Figure S49: Map illustrating the preindustrial mixed layer depth (MLD) across the Global Ocean (BIO+FPR). The MLD is mostly shallower than ~100m in low-latitude waters, but tends to be deeper in high-latitude waters and especially in regions with significant downwelling. Plot created with Panoply.

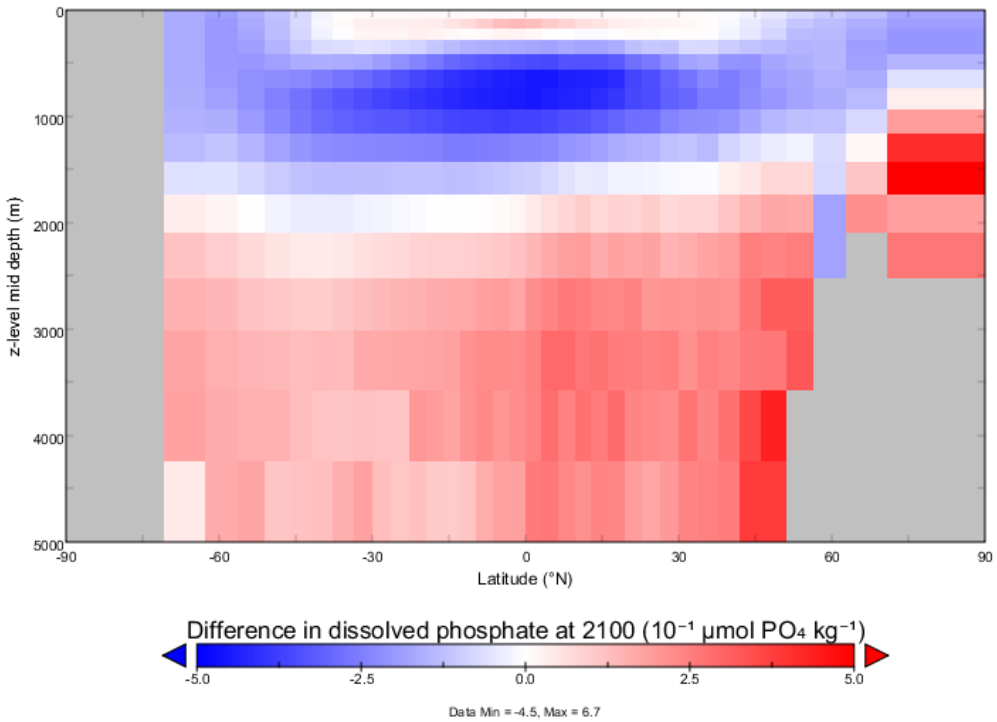

Figure S50: Depth plot of the difference in PO_4 between the recalibrated BIO+TDR and the BIO+FPR configurations under RCP 4.5 at 2100 CE. This illustrates the relative nutrient-enrichment of the layer below the surface layer in tropical regions and PO_4 depletion in polar and intermediate depth waters. N.B. recalibrated configurations are used in Section 4 to facilitate easier inter-comparison between them regardless of differing baseline conditions. Plot created with Panoply.

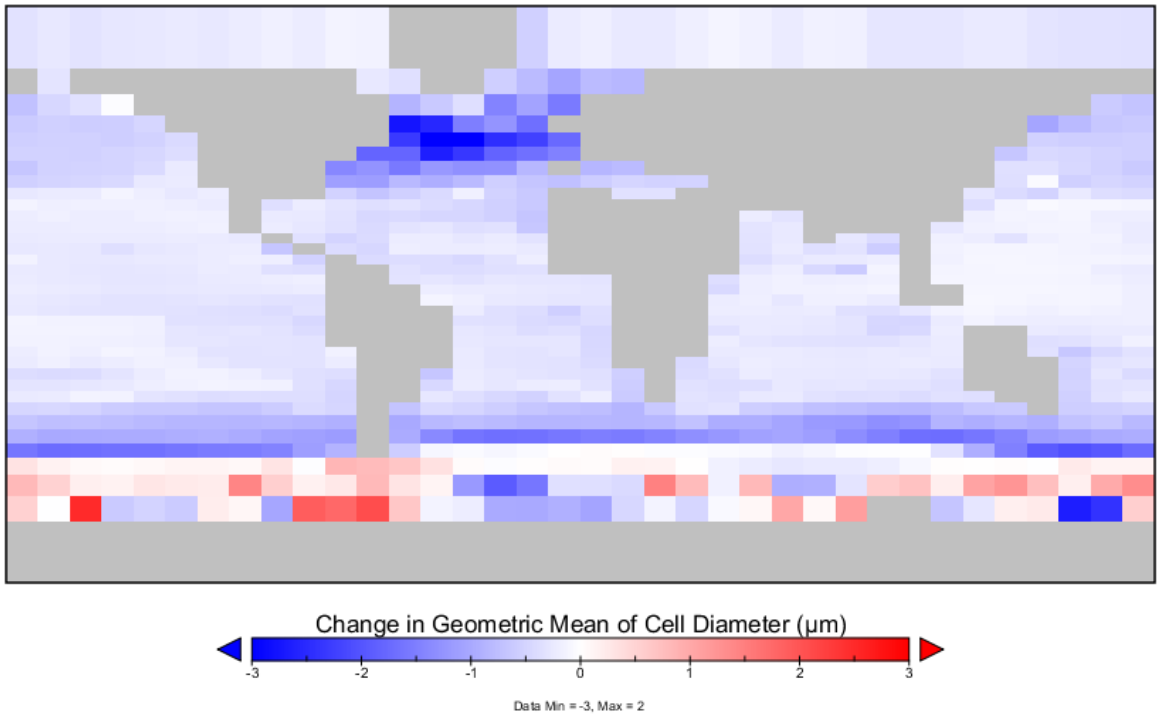

Figure S51: Map illustrating the change in mean plankton size under RCP4.5 from 1765 to 2100 CE (recalibrated ECO+FPR). Ecosystem composition shifts to smaller plankton classes across most of the Global Ocean (except parts of the Southern Ocean). Plot created with Panoply.

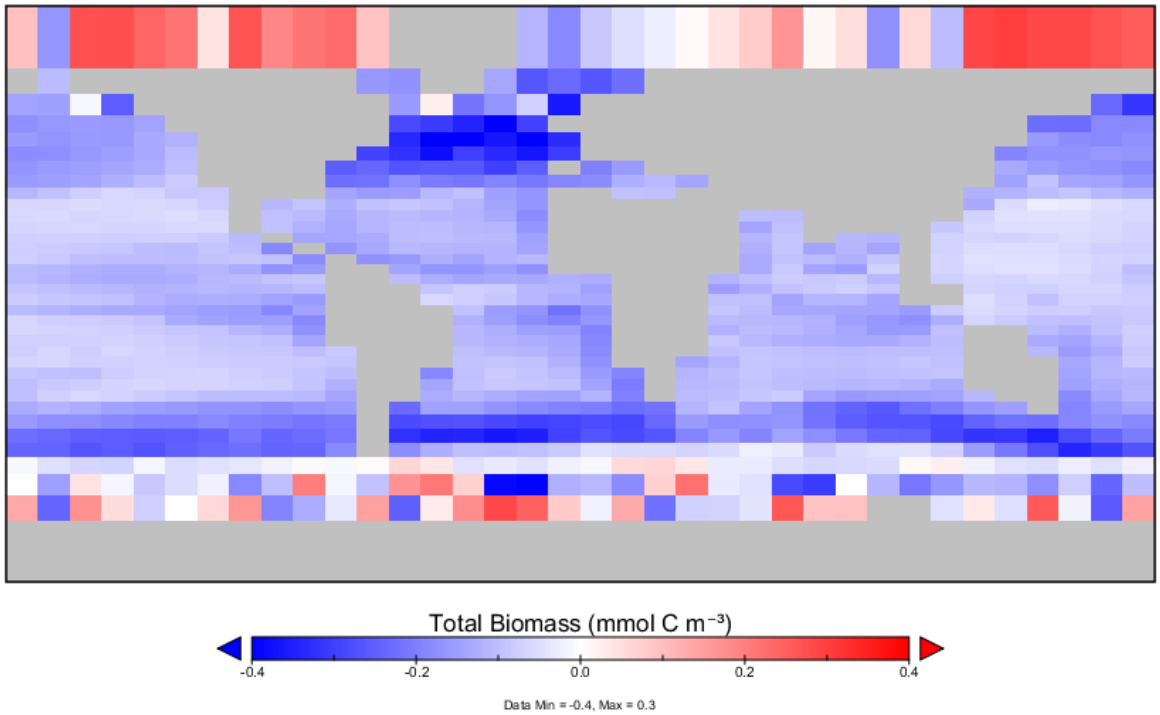

Figure S52: Map illustrating the change in total ecosystem biomass under RCP4.5 from 1765 to 2100 CE (recalibrated ECO+FPR). Biomass declines across the low and mid-latitudes, but increases in some high-latitude regions. Plot created with Panoply.

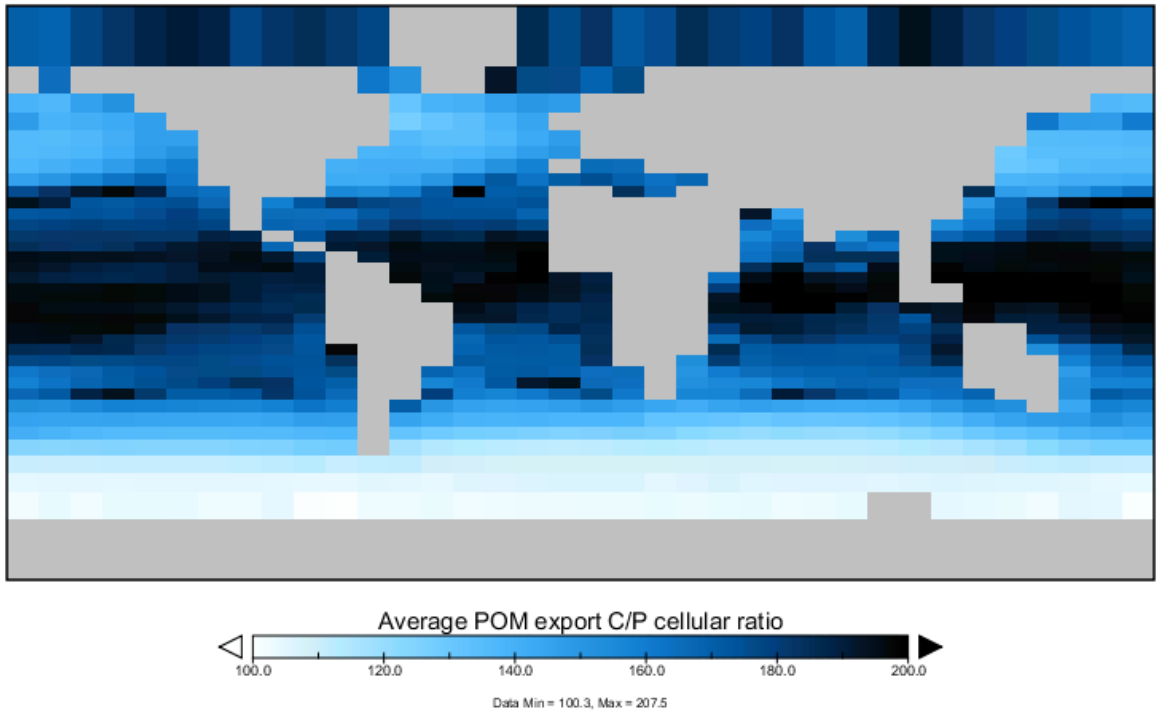

Figure S53: Map illustrating the average preindustrial ratio between carbon and phosphorus in exported POM (recalibrated ECO+FPR). The global average is higher than the canonical Redfield ratio (106:1) but matches observations (163:1), and is higher in the tropics (~200:1) and lower in the Southern Ocean (~100:1). Plot created with Panoply.

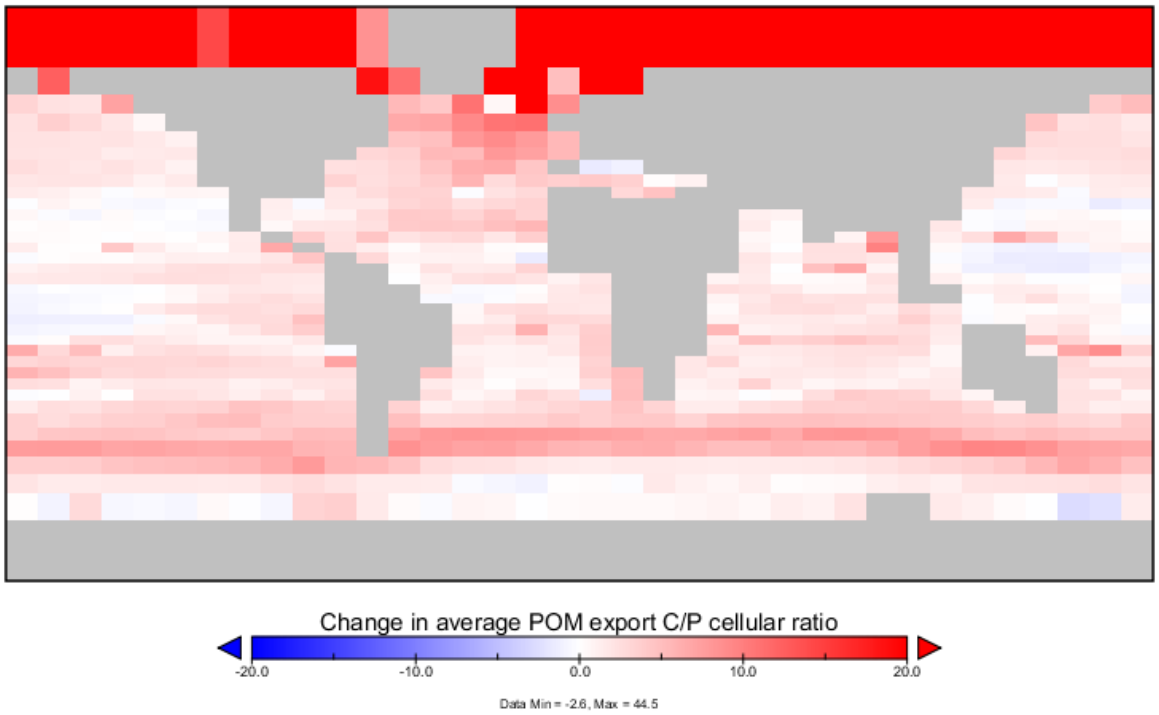

Figure S54: Map illustrating the change in the average ratio between carbon and phosphorus in exported POM under RCP4.5 from 1765 to 2100 CE (recalibrated ECO+FPR). The C:P ratio increases across most of the Global Ocean, and in particular in the Arctic Ocean. Plot created with Panoply.

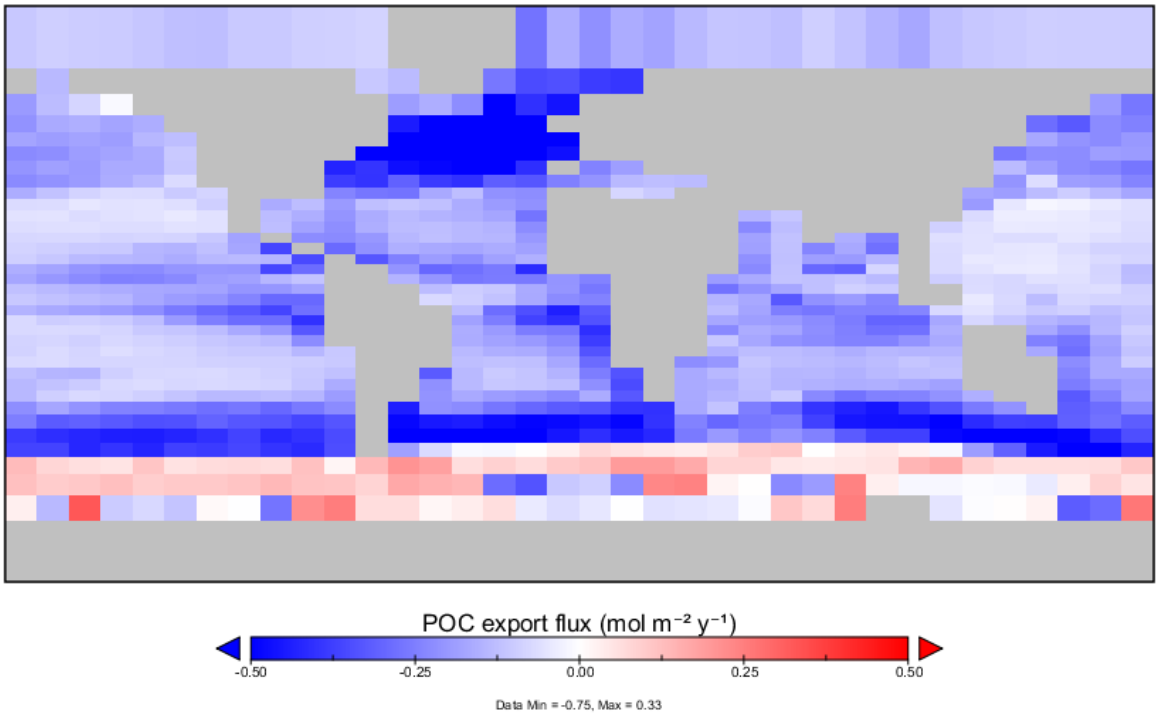

Figure S55: Map illustrating changes in POC export flux under RCP4.5 from 1765 to 2100 CE (recalibrated ECO+FPR, in contrast to the default calibration results in Figure 3c). Export falls in almost every region except for along the Antarctic Polar Front. Plot created with Panoply.

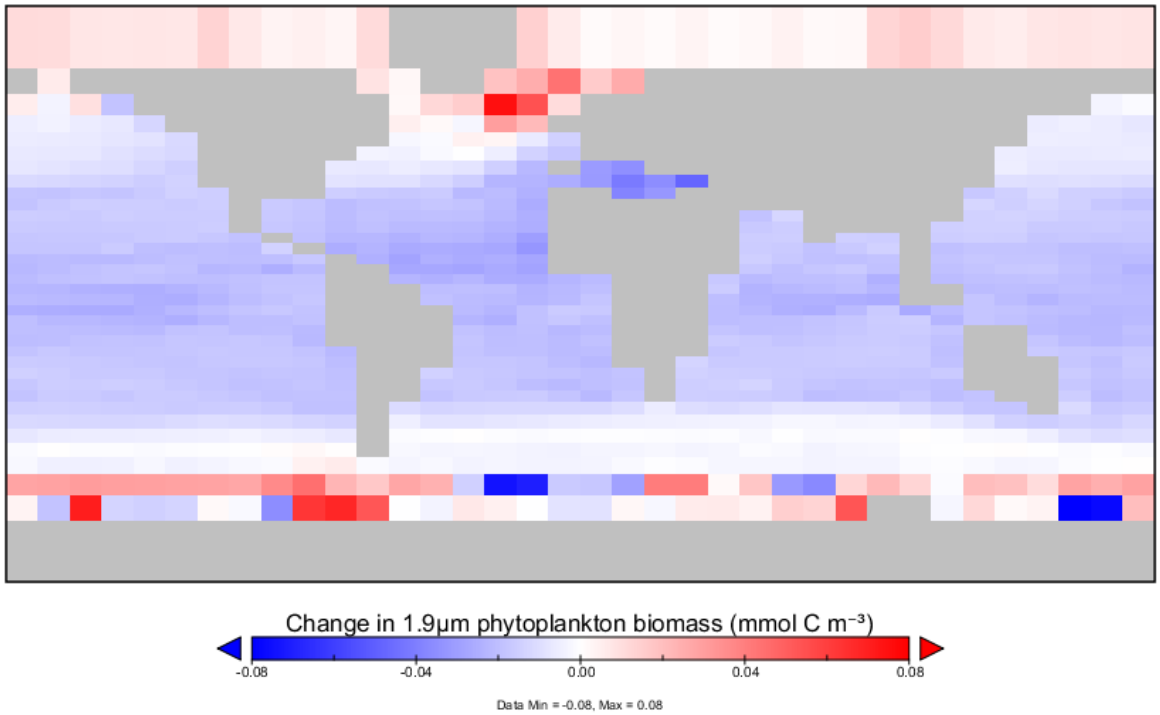

Figure S56: Map illustrating changes in phytoplankton biomass in the 1.9µm size class under RCP4.5 from 1765 to 2100 CE (recalibrated ECO+FPR). Phytoplankton of this size class decline in the low and mid-latitudes, but increases in many high-latitude and downwelling regions. Plot created with Panoply.

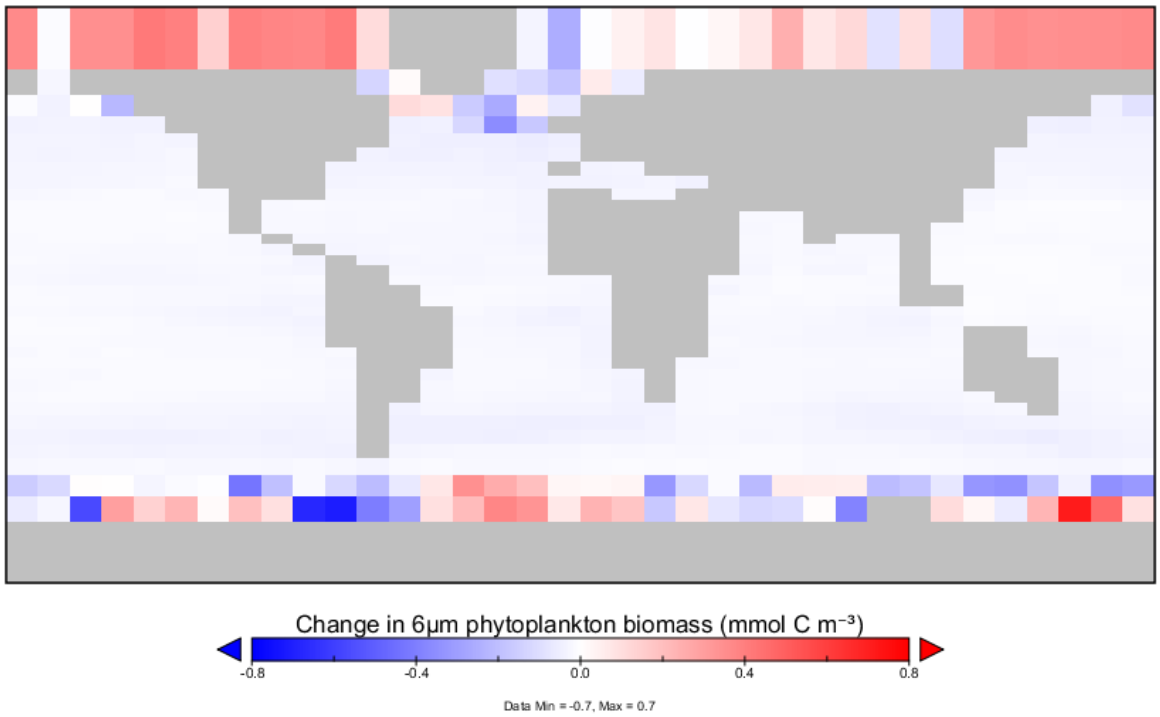

Figure S57: Map illustrating changes in phytoplankton biomass in the 6µm size class under RCP4.5 from 1765 to 2100 CE (recalibrated ECO+FPR). Phytoplankton of this size class decline in the low and mid-latitudes, but increases in many high-latitude regions. Plot created with Panoply.

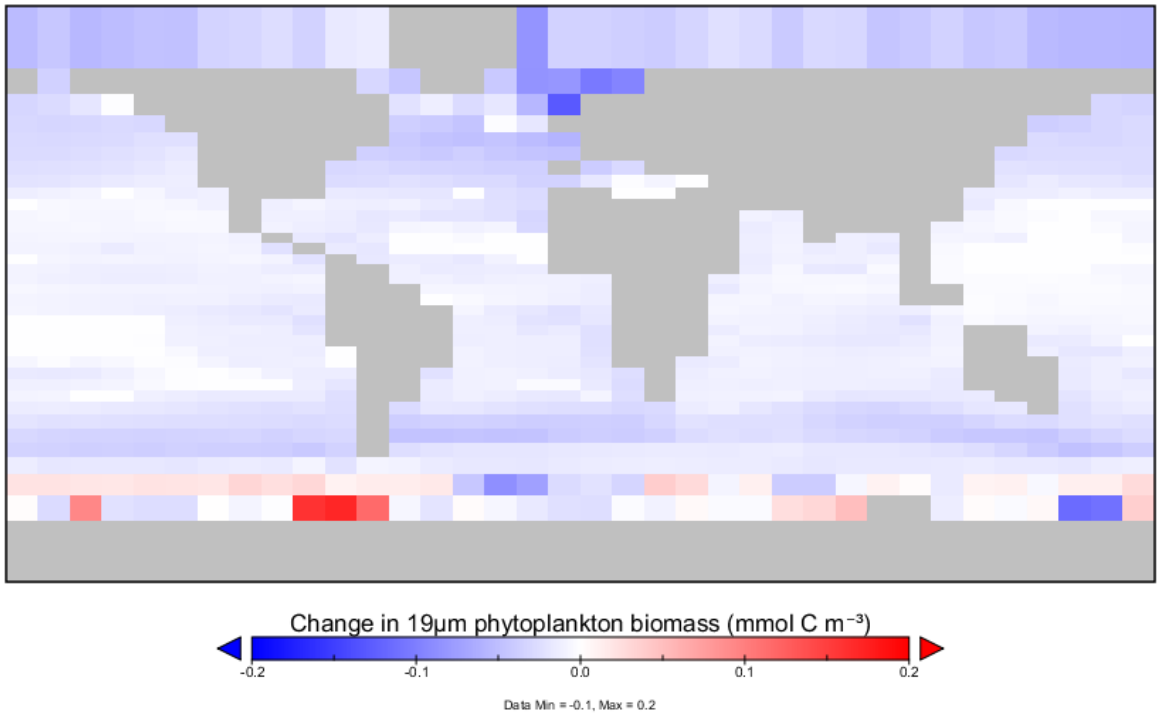

Figure S58: Map illustrating changes in phytoplankton biomass in the 19µm size class under RCP4.5 from 1765 to 2100 CE (recalibrated ECO+FPR). Phytoplankton of this size class decline in the low and mid-latitudes as well as the Arctic Ocean, but increases in parts of the Southern Ocean. Plot created with Panoply.

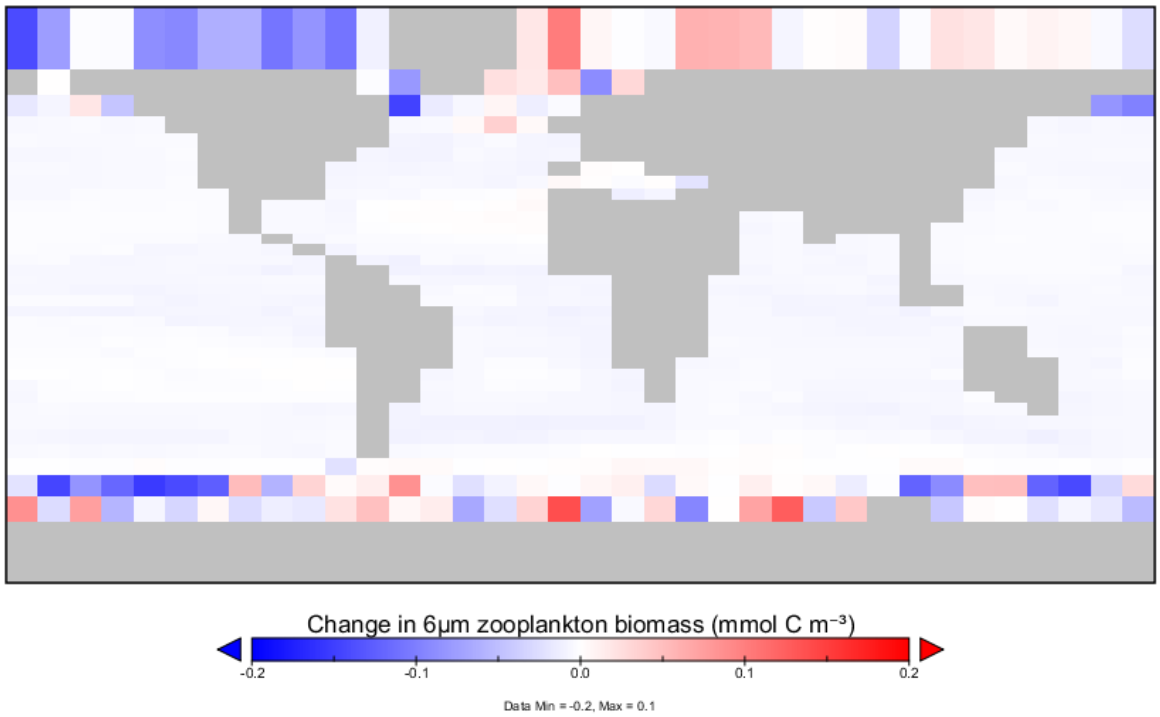

Figure S59: Map illustrating changes in phytoplankton biomass in the 6µm size class under RCP4.5 from 1765 to 2100 CE (recalibrated ECO+FPR). Zooplankton of this size class decline in the low and mid-latitudes, but increases in many high-latitude regions. Plot created with Panoply.

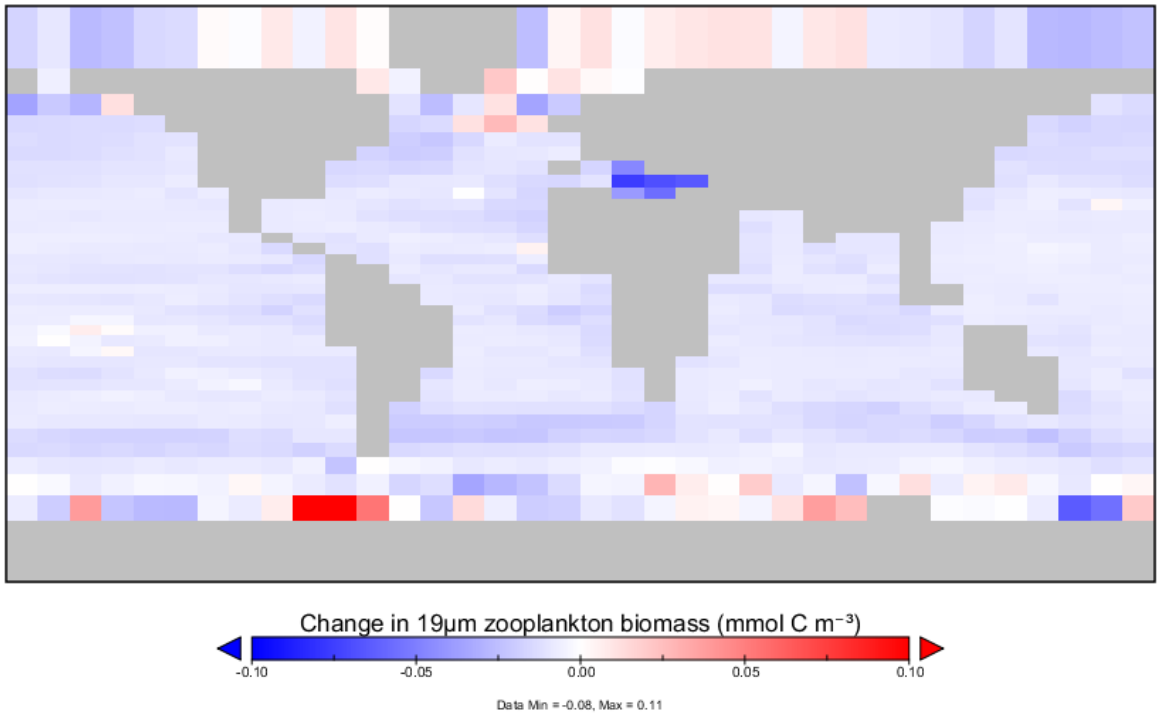

Figure S60: Map illustrating changes in phytoplankton biomass in the 19µm size class under RCP4.5 from 1765 to 2100 CE (recalibrated ECO+FPR). Zooplankton of this size class decline in the low and mid-latitudes, but increases in many high-latitude regions. Plot created with Panoply.

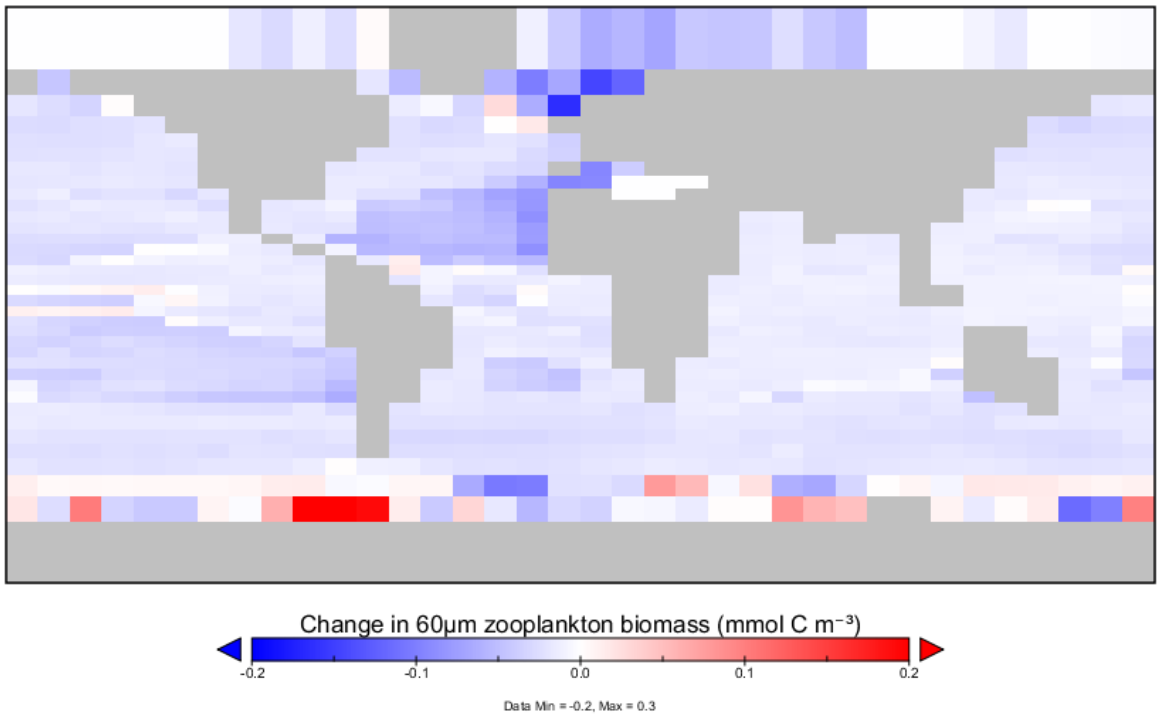

Figure S61: Map illustrating changes in phytoplankton biomass in the 60µm size class under RCP4.5 from 1765 to 2100 CE (recalibrated ECO+FPR). Zooplankton of this size class decline in the low and mid-latitudes as well as the Arctic Ocean, but increases in parts of the Southern Ocean. Plot created with Panoply.

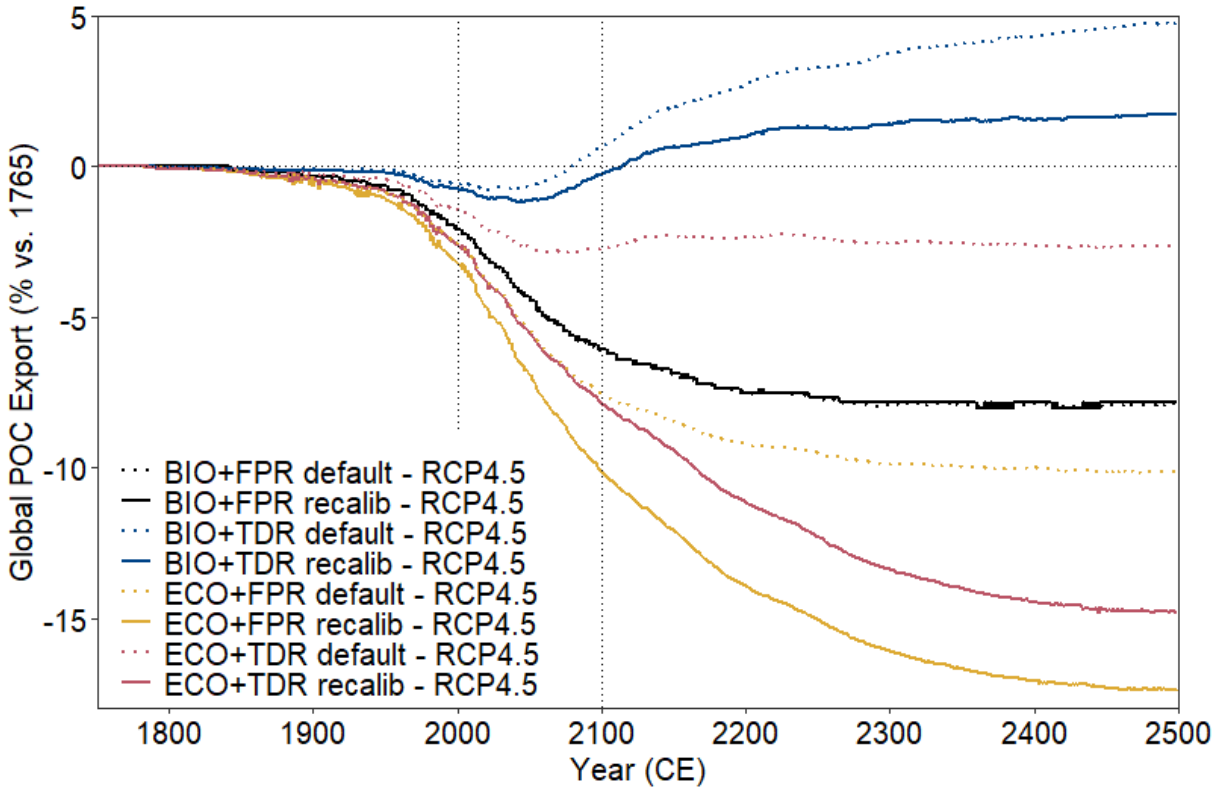

Figure S62: Graph illustrating the impact of our recalibrations on POC export across the four configurations under RCP4.5. Default calibrations (dotted lines) have a reduced decline or enhanced increase in POC export relative to the recalibrations (solid lines) for BIO+TDR (blue), ECO+FPR (yellow), and ECO+TDR (red). However, these default calibrations have substantially different baseline biological pumps than BIO+FPR, while the ECO recalibrations have much higher POC recalcitrant fractions, making them difficult to directly compare.

4.3. *Ocean Carbon Sink Capacity*

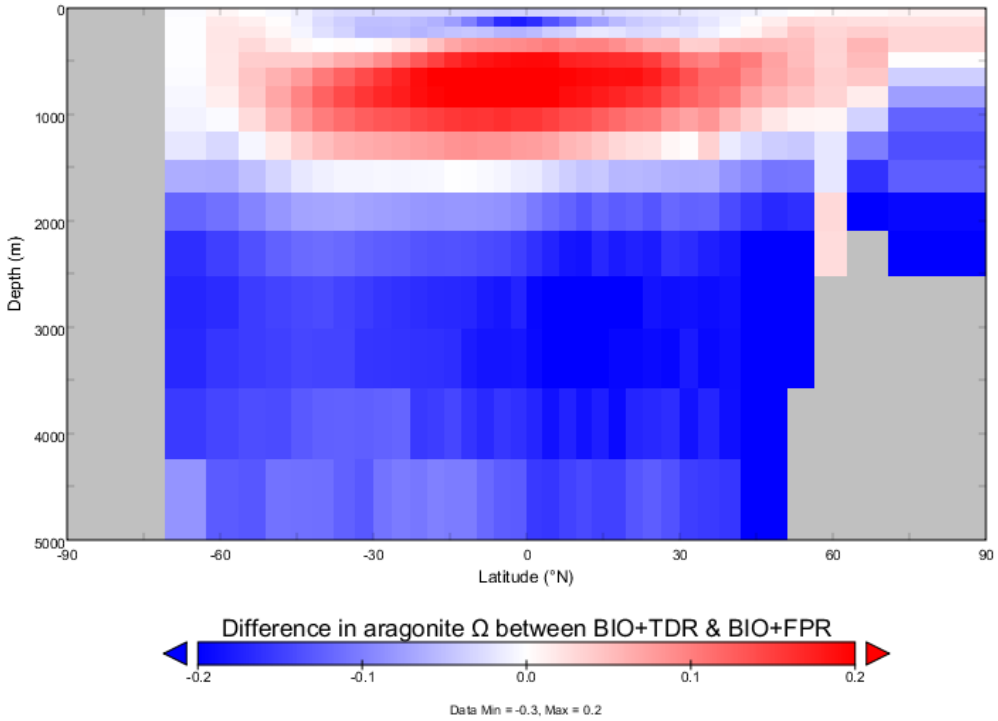

Figure S63: Depth plot illustrating difference in aragonite saturation state (Ω) between the recalibrated BIO+TDR and the BIO+FPR configurations under RCP 4.5 at 2100 CE. Increased surface remineralisation and POC export lead to reduced [CO_3] and Ω in surface waters and conversely elevated values for these in intermediate waters. In combination with shallower DIC remineralisation this leads to higher surface pCO_2, which then decreases the air-to-sea CO_2 flux and the global ocean carbon sink capacity. Plot created with Panoply.

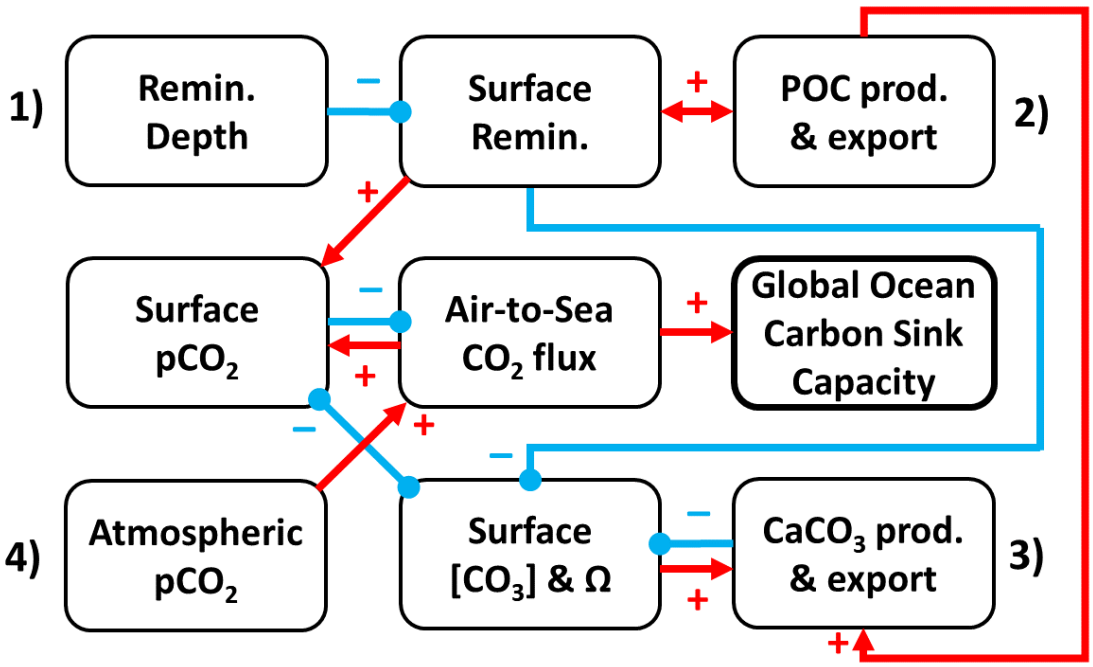

Figure S64: Schematic illustrating the effect of changes in remineralisation and production on the global ocean carbon sink capacity in our results. Blue dot-ended arrows indicate a negative effect (e.g. increased remineralisation depth leads to decreased surface remineralisation) and red point-ended arrows indicate a positive effect (e.g. increased surface remineralisation leads to increased surface pCO_2). Four pathways are described in the manuscript and labelled here: 1) shoaled (decreased) remineralisation depth and 2) increased production increasing surface remineralisation and surface pCO_2 and therefore reducing Air-to-Sea CO_2 flux; 3) increased $CaCO_3$ production and surface remineralisation reduce surface omega and therefore increase surface pCO_2; and 4) increased atmospheric pCO_2 directly increases surface pCO_2 (ocean acidification).

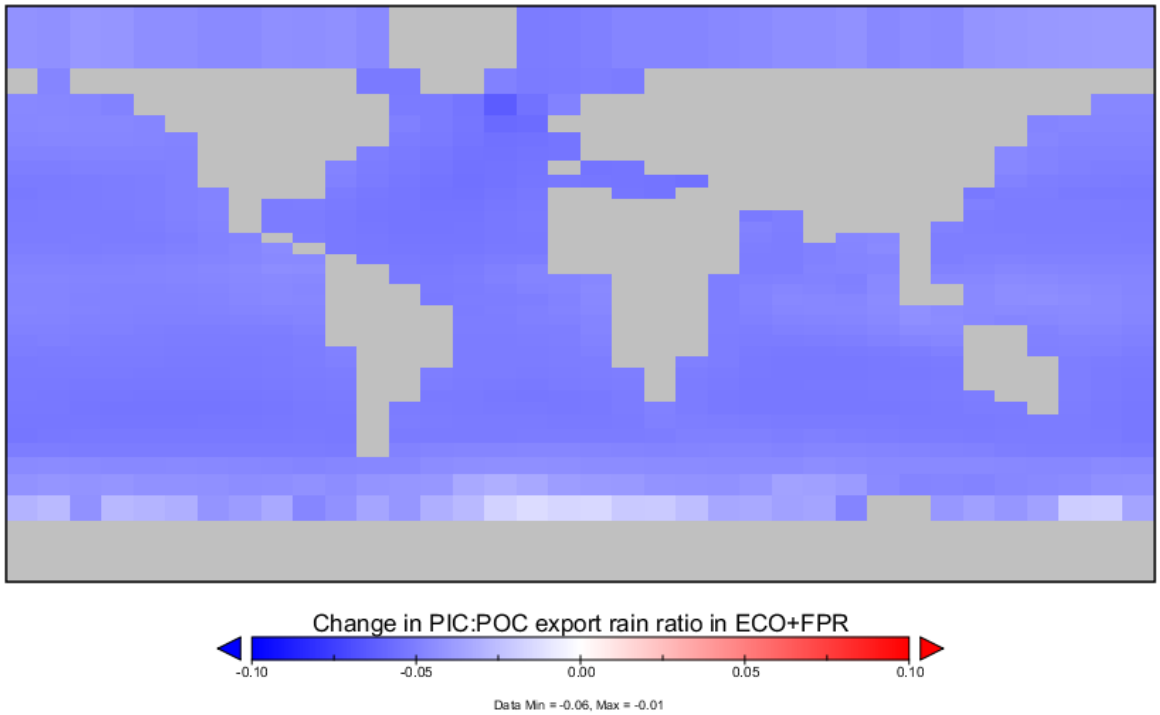

Figure S65: Map illustrating the change in PIC:POC export rain ratio under RCP4.5 from 1765 to 2100 CE (recalibrated ECO+FPR). PIC relative to POC export falls relatively uniformly (~0.03 vs. mean ~0.09) as a result of ocean acidification, except parts of the Southern Ocean where PIC production is already minimal due to low Ω. Plot created with Panoply.

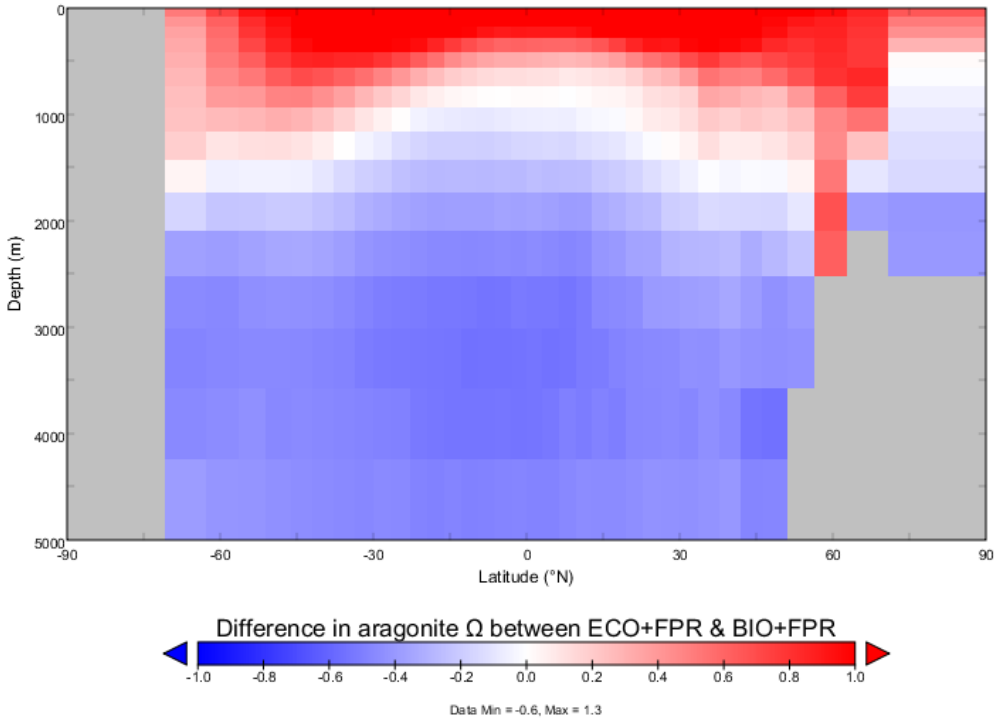

Figure S66: Depth plot illustrating difference in aragonite saturation state (Ω) between the recalibrated ECO+FPR and the BIO+FPR configurations under RCP 4.5 at 2100 CE. Decreased surface remineralisation and PIC export lead to elevated [CO_3] and Ω in surface waters and conversely reduced values for these in intermediate and deep waters. This leads to lower surface pCO_2, which then increases the air-to-sea CO_2 flux and the global ocean carbon sink capacity. Plot created with Panoply.

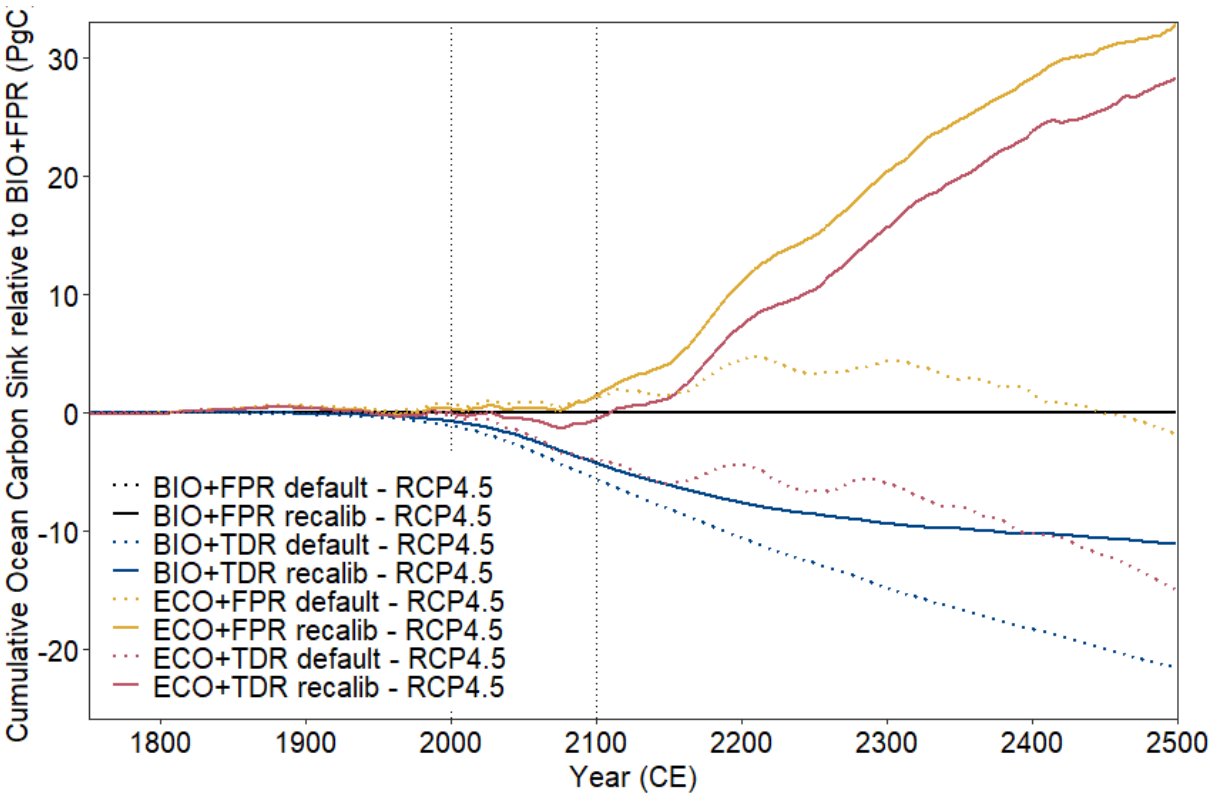

Figure S67: Graph illustrating the impact of our recalibrations on the cumulative ocean carbon sink relative to BIO+FPR across the four configurations under RCP4.5. Default calibrations (dotted lines) have stronger declines or weaker increases in carbon sink capacity relative to the recalibrations (solid lines) for BIO+TDR (blue), ECO+FPR (yellow), and ECO+TDR (red). However, these default calibrations have substantially different baseline biological pumps and surface carbonate chemistry than BIO+FPR, while the ECO recalibrations have much higher POC recalcitrant fractions, making them difficult to directly compare.

References

Garcia, H. E., Locarnini, R. A., Boyer, T. P., Antonov, J. I., Zweng, M. M., Baranova, O. K. and Johnson, D. R.: World Ocean Atlas 2009, Volume 4: Nutrients (phosphate, nitrate, and silicate), NOAA World Ocean Atlas, 71(March), 398 [online] Available from: http://www.nodc.noaa.gov/OC5/indprod.html, 2010.

NASA Goddard Space Flight Center: Sea-viewing Wide Field-of-view Sensor (SeaWiFS) Chlorophyll Data; 2014 Reprocessing, Greenbelt, MD, USA. [online] Available from: https://oceancolor.gsfc.nasa.gov/data/10.5067/ORBVIEW-2/SEAWIFS/L3B/CHL/2018/, 2015.

Olsen, A., Key, R. M., Van Heuven, S., Lauvset, S. K., Velo, A., Lin, X., Schirnick, C., Kozyr, A., Tanhua, T., Hoppema, M., Jutterström, S., Steinfeldt, R., Jeansson, E., Ishii, M., Pérez, F. F. and Suzuki, T.: The global ocean data analysis project version 2 (GLODAPv2) - An internally consistent data product for the world ocean, Earth Syst. Sci. Data, 8(2), 297–323, doi:10.5194/essd-8-297-2016, 2016.

Ward, B. A., Wilson, J. D., Death, R. M., Monteiro, F. M., Yool, A. and Ridgwell, A.: EcoGEnIE 1.0: plankton ecology in the cGEnIE Earth system model, Geosci. Model Dev., 11(10), 4241–4267, doi:10.5194/gmd-11-4241-2018, 2018.